SEISMIC EVALUATION OF UN-REINFORCED MASONRY STRUCTURES

A THESIS

Submitted by

DEBRANJAN SAR (611 CE 801)

In partial fulfillment of the requirements for
the award of the degree of

MASTER OF TECHNOLOGY (RESEARCH)

Department of Civil Engineering
National Institute of Technology Rourkela
Odisha -769 008, India

July 2014

THESIS CERTIFICATE

This is to certify that the thesis entitled "**SEISMIC EVALUATION OF UN-REINFORCED MASONRY STRUCTURES**" submitted by **DEBRANJAN SAR** to the National Institute of Technology Rourkela for the award of the degree of Master of Technology (Research) is a bonafide record of research work carried out by him under our joint supervision. The contents of this thesis, in full or in parts, have not been submitted to any other Institute or University for the award of any degree or diploma.

Place:
Date:

Dr. Pradip Sarkar
(Thesis Supervisor)
Associate Professor
Department of Civil Engineering
NIT Rourkela
Rourkela – 769 008

Place:
Date:

Dr. Pulak Kumar Munshi
(Thesis co-supervisor)
Technical Director
Department of Civil Engineering
MN Dastur & Co. Pvt. Ltd.
Kolkata – 700013

ACKNOWLEDGEMENTS

I would like to express my sincere gratitude to my thesis supervisor Dr. Pradip Sarkar, Department of Civil Engineering, National Institute of Technology Rourkela, for his logical guidance, endless inspiration, continuous moral support and affectionate relationship throughout the course of study. I consider myself very fortunate to get this opportunity to work under his supervision. Without his enormous support, this thesis would not have been possible.

I would also like to thank my co-supervisor Dr. Pulak K Munshi, Technical Director of MN Dastur & Co. Pvt. Ltd., Kolkata for his fruitful discussion and valuable guidance throughout my course of work.

My sincere thanks to Prof. N. Roy and Prof. S.P. Singh of National Institute of Technology Rourkela, for their suggestions and encouragement.

Above all, I am very grateful to our director Dr. Abhijit Dasgupta of my working organisation, MN Dastur & Co. Pvt. Ltd. for granting me leave and constant encouragement during my course of work.

I am very much thankful to my parents, sister and brother for their continuous support and encouragement throughout my life.

Last but not the least; I thank my colleagues and friends for their understanding, patience and inspiration

Place: **Debranjan Sar**

Date:

ABSTRACT

KEYWORDS: *Seismic evaluation, un-reinforced masonry, demand-to-capacity ratio, pushover analysis, plastic hinge, shear stress.*

It is well known that masonry buildings suffer a great deal of damage during earthquakes, leading to significant loss of lives. Almost 75% of the fatalities, attributed to earthquake in last century, is caused by collapse of buildings of which the greatest portion (more than 70%) is due to collapse of masonry buildings. A majority of the tenements in India are Unreinforced Masonry (URM) buildings that are weak and vulnerable even under moderate earthquakes. On the other hand, a cursory glance through the literature on earthquake resistant structures reveals that a bulk of research efforts is on RC structures. Clearly there is a great need to expend more effort in understanding masonry buildings subjected to earthquake induced dynamic loads.

The main aim of this thesis is to study the methodology available in literature to evaluate the seismic vulnerability of un-reinforced masonry building using linear/non-linear static and dynamic analyses and to check the applicability of these procedures for seismic evaluation of un-reinforced masonry building through experimental studies.

To achieve the above objectives an experimental program has been carried out as part of this research. Sixteen wall panels of varying dimensions were tested for in-plane monotonic lateral loads. For each specimen a constant axial compressive load was maintained during testing. A window opening at prescribed location of the test specimen was provided for eight of the sixteen specimens and its in-plane monotonic lateral load behaviour was studied. Four additional specimens with a door opening in combination with a window opening were tested

for their in-plane monotonic lateral load behaviour. Four solid walls without any opening were also tested and compared with the behaviour of similar panels with openings.

The experimental results are compared with the results of existing pushover analysis method (ASCE/SEI 41-06) for URM building. The comparisons show that ASCE/SEI 41-06 method consistently overestimates the strength and stiffness of the URM buildings. A set of modification is proposed for the pushover analysis of URM building based on the experimental investigation. These proposed modifications show consistently good performance in comparison with the existing method (ASCE/SEI 41-06) of pushover analysis.

A model seismic evaluation case study of an existing URM building from Guwahati, India (Zone V) is presented using equivalent static method and response spectrum method (IS 1893: 2002) followed by pushover analysis as per ASCE/SEI 41-06 with proposed modification.

TABLE OF CONTENTS

LIST OF TABLES

LIST OF FIGURES

ABBREVIATIONS

URM	-	Un-Reinforced Masonry
ATC	-	Applied Technology Council
CQC	-	Complete Quadratic Combination
CSM	-	Capacity Spectrum Method
DCM	-	Displacement Coefficient Method
FEMA	-	Federal Emergency Management Agency
IS	-	Indian Standard
PGA	-	Peak Ground Acceleration
RC	-	Reinforced Concrete
SAP	-	Structural Analysis Program
SDOF	-	Single Degree of Freedom
FE	-	Finite Element
SRSS	-	Square Root of Sum of Square
DCR	-	Demand to Capacity Ratio
ADRS	-	Acceleration Displacement Response Spectrum
ISMC	-	Indian Standard Medium Channel
MCE	-	Maximum Considered Earthquake
DBE	-	Design Basis Earthquake

NOTATION

English Symbols

a	-	regression constant
c	-	classical damping
C_0	-	factor for MDOF displacement
C_1	-	factor for inelastic displacement
C_2	-	factor for strength and stiffness degradation
C_3	-	factor for geometric nonlinearity
d	-	effective depth of the section
d_b	-	diameter of the longitudinal bar
d_p	-	spectral displacement corresponding to performance point
D	-	overall depth of the beam.
$D_n(t)$	-	displacement response for an equivalent SDOF system,
E_c	-	short-term modulus of elasticity of concrete
E_D	-	energy dissipated by damping
E_s	-	modulus of elasticity of steel rebar
E_S	-	maximum strain energy
E_{sec}	-	elastic secant modulus
EI	-	flexural rigidity of beam
f_c	-	concrete compressive stress
f'_{cc}	-	compressive strength of confined concrete
f'_{co}	-	unconfined compressive strength of concrete
f_{ck}	-	characteristic compressive strength of concrete
F_e	-	elastic strength
$\{f_s(t)\}$	-	lateral load vector

$\{f_{s,UB}\}$ - force vector in upper bound pushover analysis

f_y - yield stress of steel rebar

F_y - defines the yield strength capacity of the SDOF

f_{yh} - grade of the stirrup reinforcement

G - shear modulus of the reinforced concrete section

h - overall building height (in m)

k - lateral stiffness

k_e - confinement effectiveness coefficient

K_{eq} - equivalent stiffness

K_i - initial stiffness

l - length of frame element

l_p - equivalent length of plastic hinge

m - storey mass

M_n^* - modal mass for n^{th} mode

N - number of modes considered

$P_{eff}(t)$ - effective earthquake force

$q_n(t)$ - the modal coordinate for n^{th} mode

R - Regular frame considered for study

S1 - Type- 1 setback frame considered for study

S2 - Type- 2 setback frame considered for study

S3 - Type- 3 setback frame considered for study

$\{s\}$ - height-wise distribution of effective earthquake force

S_a - spectral acceleration

S_d - spectral displacement

$\{s_n\}$ - n^{th} mode contribution in $\{s\}$

SR_A - spectral reduction factor at constant acceleration region

SR_V - spectral reduction factor at constant velocity region

T - fundamental natural period of vibration

T_{eq} - equivalent time period

T_i - initial elastic period of the structure

T_n - n^{th} mode natural period

$\ddot{u}_g(t)$ - earthquake ground acceleration

$u_{n,roof}(t)$ - displacement at the roof due to n^{th} mode

$u_{no,roof}$ - peak value of the roof displacement due to n^{th} mode

$u_{roof}(t)$ - roof displacement at time 't'

[illegible] - target roof displacement in upper bound pushover analysis

V_{Bn} - base shear capacity for n^{th} mode pushover analysis

x - strain ratio

Greek Symbols

α - post-yield stiffness ratio

β_{eq} - equivalent damping

β_i - initial elastic damping

β_s - damping due to structural yielding

δ_t - target displacement

ε_{sm} - steel strain at maximum tensile stress

$\{\phi_n\}$ - n^{th} mode shape of the structure

$\phi_{n,roof}$ - value of the n^{th} mode shape at roof

φ_u - ultimate curvature

φ_y - yield curvature

κ - an adjustment factor to approximately account for changes in hysteretic behaviour in reinforced concrete structures

μ - displacement ductility ratio

θ_p - plastic rotation

θ_u - ultimate rotation

θ_y - yield rotation

ρ_s - volumetric ratio of confining steel

ω_n - n^{th} mode natural frequency

ξ_n - n^{th} mode damping ratio

Γ_n - modal participation factor of the n^{th} mode

CHAPTER 1

INTRODUCTION

1.1 BACKGROUND AND MOTIVATION

It is well known that masonry buildings suffer a great deal of damage during earthquakes. This is especially true for the unreinforced masonry (URM) buildings built in rural and semi-urban areas of developing countries. Fig. 1.1 shows a typical load bearing URM building. Many heritage buildings around the world are of old and thick walled masonry. Their value, historic, artistic, social or financial, is great and damage to them in an earthquake involves very costly repair.

Fig.1.1: Typical load bearing masonry construction for a residential building

Normally thick walled URM buildings were designed for vertical loads, since masonry has adequate compressive strength the structure behaves well as long as the loads are vertical. When such a masonry structure is subjected to lateral inertial loads during an

earthquake, the walls develop shear and flexural stresses. The strength of masonry under these conditions often depends on the bond between brick and mortar. A masonry wall can also undergo in-plane shear stresses if the lateral forces are in the plane of the wall. Shear failure in the form of diagonal cracks is observed due to this. However, catastrophic collapses take place when the wall experiences out-of-plane flexure. This can bring down a roof and cause more damage. Fig. 1.2 shows typical failure of an URM building during 2010 Haiti earthquake.

Fig.1.2: Failure of an URM building during 2010 Haiti earthquake

Masonry buildings with light roof such as tiled roof are more vulnerable to out-of-plane vibrations since the top edge can undergo large deformations, due to lack of lateral restraint. Damage to masonry buildings in earthquakes may be influenced by four general categories: quality of materials and construction, connections between structural elements, structural layout and soil-structure interaction.

1.2 OBJECTIVE OF THE THESIS

Based on the literature review presented in Chapter 2 the salient objective of this research is defined as:

i) To assess pushover analysis methodology prescribed in ASCE/SEI 41-06 for unreinforced masonry buildings through experimental investigation and to propose improvement if required

ii) To develop equivalent frame model for nonlinear analysis of URM building

iii) To carry out a case study of seismic evaluation of an existing URM building using the improved pushover analysis.

1.3 SCOPE OF THE STUDY

The present study is limited to medium strength clay brick masonry wall. Fly ash brick masonry, hollow block masonry, etc. are kept outside the scope of the present study.

URM wall with strip footing is considered in the study. In the computer model the footing is modelled with fixity.

Two-dimensional wall panels are used for experimental testing to define in-plane lateral load-deformation behaviour of the wall panel. Out-of-plane lateral strength of the wall is ignored in the present study as it is very small compared to in-plane lateral strength

1.4 METHODOLOGY

The steps undertaken in the present study to achieve the above-mentioned objectives are as follows:

a) Carry out extensive literature review, to establish the objectives of the research work.

b) Develop a computer model with nonlinear line elements to represents unreinforced masonry wall.

c) Carry out experimental program for following three types of masonry walls with varying dimensions: (i) solid wall, (ii) wall with window opening and (iii) wall with door and window opening to obtain lateral force versus top displacement relation.

d) Carry out nonlinear static (pushover) analyses of above mentioned different wall panels as per the proposed model with line elements considering nonlinear hinges as defined by ASCE/SEI 41-06.

e) Compare the lateral load deformation behaviour of the selected wall panels obtained from experimental investigation and pushover analysis.

f) Propose improved nonlinear hinge model to carry out nonlinear analysis of unreinforced masonry wall if required.

g) Carry out a detailed case study of pushover analysis on a typical unreinforced masonry building with proposed modelling approach and nonlinear hinges, if any.

1.5 ORGANISATION OF THE THESIS

This introductory chapter has presented the background, objective, scope and methodology of the present study. Chapter 2 starts with a description of the previous work done on unreinforced masonry wall by other researchers. Later in the chapter, a description of the pushover analysis procedure as per ASCE/SEI 41-06 is presented.

Chapter 3 describes the analytical modelling used in the present study for representing the actual behaviour of unreinforced masonry wall.

Chapter 4 begins with a presentation of experimental program including the description of wall samples and experimental procedures. The next part of this chapter presents load deformation results obtained from the experimental investigation. Finally, this chapter presents and compares the nonlinear static analysis (pushover) results carried out for the same wall specimens with the experimental results. This also includes the discussions on proposed modifications on the nonlinear hinge models for unreinforced masonry wall.

Chapter 5 presents a detailed case study of pushover analysis on a typical unreinforced masonry building through step by step procedures using proposed modification for structural modelling.

Finally, Chapter 6 presents a summary including salient features, significant conclusions from this study and the future scope of research in this area.

CHAPTER 2

LITERATURE REVIEW

2.1 INTRODUCTION

The first half of this chapter is devoted to a review of published literature on unreinforced masonry (URM) buildings. This part describes a number of experimental and analytical works on unreinforced masonry buildings.

The second half of this chapter is devoted to a review of seismic evaluation methods available in literature. This includes different evaluation methods based on linear and nonlinear analyses. Pushover analysis is an important tool for the seismic evaluation of buildings. A description of traditional pushover analysis procedures as per ASCE/SEI 41-06 is presented at the end of this chapter.

2.2 RESEARCH ON URM BUILDINGS

There are a number of research papers and design guidelines found on the structural properties of unreinforced masonry buildings

A number of studies were carried out by Jai Krishna and Chandra (1965) and Jai Krishna *et. al.* (1966). They studied the static in-plane strength of walls with and without reinforcement. They carried out the building analysis by considering the shear walls alone, with different parameters such as the aspect ratio of shear walls and size and location of openings in shear walls.

Arioglu and Anadol (1973) refer to the several earthquakes in Turkey and point out that plain masonry buildings are most vulnerable to earthquake damage. They refer to the special indigenous technique of producing horizontal wooden reinforcement on both faces at some

vertical intervals to prevent collapse of masonry structures. Such practices have been traditionally in vogue in Turkey.

Abrams (1992) examines the in-plane lateral load behaviour of un-reinforced masonry elements under monotonic and cyclic loading. He argues that although masonry is considered to be brittle it has considerable deformation capacity after the development of first crack. Several suggestions have been made to evaluate the masonry strength characteristics under seismic loading.

Bruneau (1994) makes a number of observations on the seismic performance of un-reinforced masonry buildings (URM). Some of the types of failures are listed as

a) Lack of anchorage between floor and walls
b) Anchor failure when joists are anchored to walls
c) In-plane failure
d) Out-of-plane failure
e) Combined in-plane

Among these he emphasis that URM buildings are most vulnerable to flexural our-of-plane failure. In-plane failure may not right away lead to collapse since the load carrying capacity of a wall is not completely lost by diagonal cracking. However, our-of-plane failure leads to unstable and explosive collapse. Sometimes an initial in-plane failure may weaken the wall and subsequent out-of-plane motion can lead to collapse.

Rai and Goel (1996) also studied the seismic strengthening of un-reinforced masonry piers with steel elements. They considered the in-plane behaviour of masonry piers. The strengthening system showed significant improvement in stiffness and ductility.

Scrivener (1996) has done a survey of the damage to old masonry buildings in earthquakes around the world. He also reported the cause of the damage under four headings: quality of materials and construction, connections between structural elements, structural layout and soil-structure interaction.

Tomazevic (1999) and his colleagues carried out a large number of Earthquake Resistant Masonry Structures. He has discussed a number of concepts for designing earthquake resistant masonry and for retrofitting partially damaged masonry structures. The following concepts may be mentioned;

a) Traditional stone masonry walls with horizontal RC bond beams connecting the walls around the building at vertical spacing of 1.0 m or 2.0 m depending on the expected seismic intensity.
b) Masonry confined in its own plane by RC bond beams and columns. The columns have to be connected to the walls through shear keys. The spacing of columns is not more than 4.0 m.
c) Vertical reinforcement is provided n grouted holes of hollow block masonry and small pockets inside brick masonry. Horizontal reinforcements in the shape of truss like arrangements are also provided in bed joints. There are Euro code specifications for such reinforcements.
d) Horizontal tie rods are provided as a retrofitting measure in grooves cut in the mortar, below the floor level, on both sides of a wall. They are anchored to steel plates at both ends of the wall.

A steel mesh is anchored to the walls on the faces and covered with plaster.

A report by Navalli (2001) refers to the practice Uttaranchal where they use horizontal timber bands at different level improve the integrity of the masonry structure. Such houses suffered little damage during the October 1991 Uttarkashi earthquake. The paper by Jai Krishna and Arya (1962) also refers to such practices.

This section, however, discusses the previous research work on the lateral load behaviour of URM buildings. Andreas *et. al.* (2002) discussed the analysis of un-reinforced masonry buildings, and also discussed, and under what conditions, a simple equivalent frame model can be used for assessment purposes. Several parametric analyses involving finite element (FE) models of two-dimensional and three-dimensional structures have been performed in the elastic range, using both refined and coarse planar meshes.

Bulk of publication on earthquake resistance of structures deals with RC structures. There have been quite a few publications on earthquake resistant of masonry structures, from different parts of the world. A representative list of publications on such masonry is discussed here.
Unreinforced Masonry Buildings and Earthquakes (FEMA P-774) described the risk assessment and guidelines how to minimise the risk of failure for existing URM Building in the year 2009 in California.

Bilgin and Korini (2012) examined the reason and capacity to failure by earthquake at Albania for the pre-defined template residential building. They carried out mainly three template building and analysed accordingly to FEMA440 guideline.

2.3 SEISMIC EVALUATION METHODS

The following are the methods recommended for detailed seismic evaluation of buildings: (i) Linear static analysis – Equivalent static analysis, (ii) Linear dynamic analysis – Response spectrum analysis and (iii) Non-linear static analysis – Push-over analysis. It is recommended that all the above methods be performed sequentially for a proper assessment of the seismic vulnerability in a building. It may be noted that more rigorous analysis (nonlinear dynamic time-history analysis) is possible, but this is not recommended as it is more involved and time consuming and not recommended for normal building. This section briefly explains the linear static and linear dynamic analyses as recommended in Indian Standard IS 1893: 2002. The main purpose of these analyses, from the seismic evaluation perspective, is to check the demand-to-capacity ratios of the building components and thereby ascertain code compliance. The non-linear static analysis (pushover analysis) is explained in the next section. The two different linear analysis methods recommended in IS 1893: 2002 are explained in this Section. Any one of these methods can be used to calculate the expected seismic demands on the lateral load resisting elements.

2.3.1 Equivalent Static Method

In the equivalent static method, the lateral force equivalent to the design basis earthquake is applied statically. The equivalent lateral forces at each storey level are applied at the floor level. The base shear ($V = V_B$) is calculated as per Clause 7.5.3 of IS 1893: 2002.

$$V_B = A_h W \tag{2.1}$$

$$A_h = \left(\frac{Z}{2}\right) \frac{I}{R} \frac{S_a}{g} \tag{2.2}$$

where $W \equiv$ seismic weight of the building, $Z \equiv$ zone factor, $I \equiv$ importance factor,

$R \equiv$ response reduction factor, $S_a/g \equiv$ spectral acceleration coefficient determined from Fig. 2.1, corresponding to an approximate time period (T_a) which is given by

$$T_a = 0.075h^{0.75} \text{ for RC moment resisting frame without masonry infill} \qquad (2.3a)$$

$$T_a = \frac{0.09h}{\sqrt{d}} \text{ for RC moment resisting frame with masonry infill} \qquad (2.3b)$$

The base dimension of the building at the plinth level along the direction of lateral forces is represented as d (in metres) and height of the building from the support is represented as h (in metres). The response spectra functions can be calculated as follows:

For Type I soil (rock or hard soil sites):
$$\frac{S_a}{g} = \begin{cases} 1+15T & 0.00 \le T \le 0.10 \\ 2.50 & 0.10 \le T \le 0.40 \\ \dfrac{1}{T} & 0.40 \le T \le 4.00 \end{cases}$$

For Type II soil (medium soil):
$$\frac{S_a}{g} = \begin{cases} 1+15T & 0.00 \le T \le 0.10 \\ 2.50 & 0.10 \le T \le 0.55 \\ \dfrac{1.36}{T} & 0.55 \le T \le 4.00 \end{cases}$$

For Type III soil (soft soil):
$$\frac{S_a}{g} = \begin{cases} 1+15T & 0.00 \le T \le 0.10 \\ 2.50 & 0.10 \le T \le 0.67 \\ \dfrac{1.67}{T} & 0.67 \le T \le 4.00 \end{cases}$$

The design base shear is to be distributed along the height of building as per Clause 7.7.1 of IS 1893: 2002.

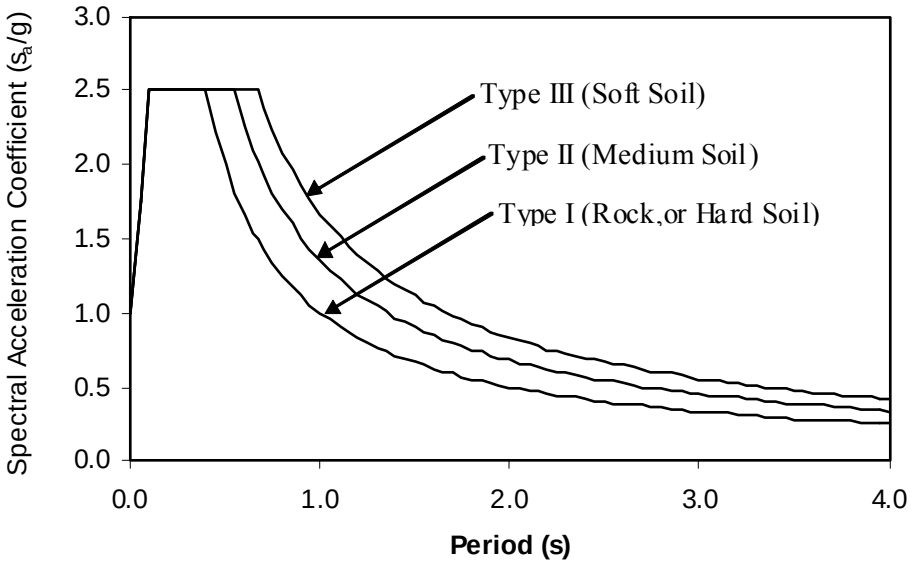

Fig. 2.1: Response spectra for 5 percent damping (IS 1893: 2002)

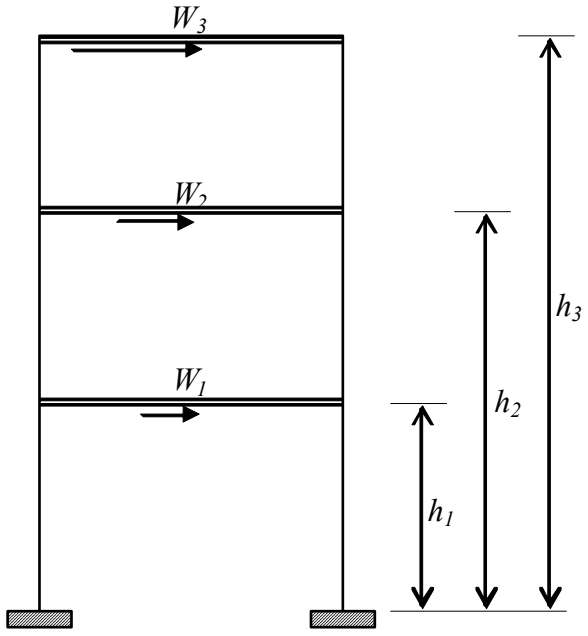

Fig. 2.2: Building model under seismic load

The design lateral force at floor *i* is given as follows

$$Q_i = V_B \frac{W_i h_i^2}{\sum_{j=1}^{n} W_i h_i^2} \tag{2.4}$$

Here $W_i \equiv$ Seismic weight of floor i, $h_i \equiv$ Height of floor measured from base,

$n \equiv$ Number of storeys in the building equal to the number of levels at which masses are located (Fig. 2.2).

2.3.2 Response spectrum analysis

The equations of motion associated with the response of a structure to ground motion are given by:

$$\mathbf{M\ddot{u}}(t) + \mathbf{C\dot{u}}(t) + \mathbf{Ku}(t) = \mathbf{m_x}\ddot{u}_{gx}(t) + \mathbf{m_x}\ddot{u}_{gy}(t) + \mathbf{m_x}\ddot{u}_{gz}(t) \tag{2.5}$$

Here, **M** is the diagonal mass matrix, **C** is the proportional damping matrix, **K** is the stiffness matrix, $\mathbf{\ddot{u}}$, $\mathbf{\dot{u}}$ and $\mathbf{u}$ are the relative (with respect to the ground) acceleration, velocity and displacement vectors, respectively, $\mathbf{m_x}$, $\mathbf{m_y}$, and $\mathbf{m_z}$ are the unit acceleration loads and $\ddot{u}_{gx}$, $\ddot{u}_{gy}$ and $\ddot{u}_{gz}$ are the components of uniform ground acceleration.

The objective of response spectrum analysis is to obtain the likely maximum response from these equations. The earthquake ground acceleration in each direction is given as a response spectrum curve. The response spectrum is a plot of the maximum response (maximum displacement, velocity, acceleration or any other quantity of interest) to a specified load function for all possible single degree-of-freedom systems. The abscissa of the spectrum is the natural period (or frequency) of the system and the ordinate is the maximum response. It is also a function of

damping. Fig.2.1 shows the design response spectra given in IS 1893: 2002 for a 5% damped system. According to IS 1893: 2002, high rise and irregular buildings must be analysed by the response spectrum method. However, this method of linear dynamic analysis is also recommended for regular buildings.

Response spectrum analysis is performed using mode superposition, where free vibration modes are computed using eigenvalue analysis. The maximum modal response (λ_k) of a quantity (considering the mass participation factor) is obtained for each mode of all the modes considered. Sufficient modes (r) to capture at least 90% of the participating mass of the building (in each of the orthogonal horizontal directions), have to be considered in the analysis. The modal responses of all the individual modes are then combined together using either the square root of the sum of the squares (SRSS) method or complete quadratic combination (CQC) method. The SRSS method is based on probability theory and is expressed as follows.

$$\lambda = \sqrt{\sum_{k=1}^{r} (\lambda_k)^2} \tag{2.6}$$

If the building has very closely spaced modes then the CQC method is preferable.

The base shear is calculated for response spectrum analysis in the following manner. The S_a/g value corresponding to each period of all the considered modes is first calculated from Fig. 2.1. The base shear corresponding to a mode is then calculated as per the design code. Each base shear is multiplied with the corresponding mass participation factor and then combined as per the selected mode combination method, to get the total base shear of the building.

If the base shear calculated from the response spectrum analysis ($\bar{V}_B$) is less than the design base shear (V_B) calculated from Equation 2.1, then as per IS 1893: 2002, all the response quantities (member forces, displacements, storey shears and base reactions) have to be scaled up by the factor $V_B / \bar{V}_B$.

2.3.3 Evaluation Results

The demands (moments, shears and axial forces) obtained at the critical sections from the linear analyses are compared with the capacities of the individual elements. The capacities of RC members are to be calculated as per IS 456: 2000. The demand-to-capacity ratio (DCR) for each element should be less than 1.0 for code compliance. For a beam, positive and negative bending moment demands at the face of the supports and the positive moment demands at the span need to be compared with the corresponding capacities. For a column, the moment demand due to bi-axial bending under axial compression must be checked using the P-M_x-M_y surface (interaction surface), generated according to IS 456: 2000.

2.4 PUSHOVER ANALYSIS – AN OVERVIEW

The use of the nonlinear static analysis (pushover analysis) came in to practice in 1970's but the potential of the pushover analysis has been recognized for last 10-15 years. This procedure is mainly used to estimate the strength and drift capacity of existing structure and the seismic demand for this structure subjected to selected earthquake. This procedure can be used for checking the adequacy of new structural design as well. The effectiveness of pushover analysis and its computational simplicity brought this procedure in to several seismic guidelines

(ATC 40, FEMA 356 and ASCE/SEI 41-06) and design codes (Eurocode 8 and PCM 3274) in last few years.

Pushover analysis is defined as an analysis wherein a mathematical model directly incorporating the nonlinear load-deformation characteristics of individual components and elements of the building shall be subjected to monotonically increasing lateral loads representing inertia forces in an earthquake until a 'target displacement' is exceeded. Target displacement is the maximum displacement (elastic plus inelastic) of the building at roof expected under selected earthquake ground motion. Pushover analysis assesses the structural performance by estimating the force and deformation capacity and seismic demand using a nonlinear static analysis algorithm. The seismic demand parameters are global displacements (at roof or any other reference point), storey drifts, storey forces, component deformation and component forces. The analysis accounts for geometrical nonlinearity, material inelasticity and the redistribution of internal forces. Response characteristics that can be obtained from the pushover analysis are summarised as follows:

a) Estimates of force and displacement capacities of the structure. Sequence of the member yielding and the progress of the overall capacity curve.

b) Estimates of force (axial, shear and moment) demands on potentially brittle elements and deformation demands on ductile elements.

c) Estimates of global displacement demand, corresponding inter-storey drifts and damages on structural and non-structural elements expected under the earthquake ground motion considered.

d) Sequences of the failure of elements and the consequent effect on the overall structural stability.

e) Identification of the critical regions, where the inelastic deformations are expected to be high and identification of strength irregularities (in plan or in elevation) of the building.

Pushover analysis delivers all these benefits for an additional computational effort (modelling nonlinearity and change in analysis algorithm) over the linear static analysis. Step by step procedure of pushover analysis is discussed next.

2.4.1 Pushover Analysis Procedure

Pushover analysis is a static nonlinear procedure in which the magnitude of the lateral load is increased monotonically maintaining a predefined distribution pattern along the height of the building (Fig. 2.3a). Building is displaced till the 'control node' reaches 'target displacement' or building collapses. The sequence of cracking, plastic hinging and failure of the structural components throughout the procedure is observed. The relation between base shear and control node displacement is plotted for all the pushover analysis (Fig. 2.3b). Generation of base shear – control node displacement curve is single most important part of pushover analysis. This curve is conventionally called as pushover curve or capacity curve. The capacity curve is the basis of 'target displacement' estimation as explained in Section 2.4.3. So the pushover analysis may be carried out twice: (a) first time till the collapse of the building to estimate target displacement and (b) next time till the target displacement to estimate the seismic demand. The seismic demands for the selected earthquake (storey drifts, storey forces, and component deformation and forces) are calculated at the target displacement level. The seismic demand is

then compared with the corresponding structural capacity or predefined performance limit state to know what performance the structure will exhibit. Independent analysis along each of the two orthogonal principal axes of the building is permitted unless concurrent evaluation of bi-directional effects is required.

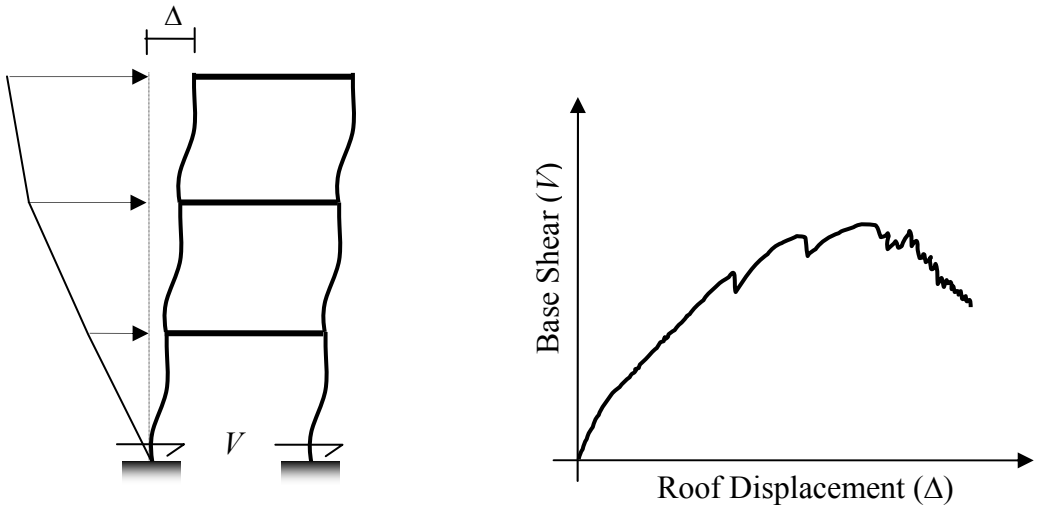

a) Building model b) Pushover curve

Fig. 2.3: Schematic representation of pushover analysis procedure

The analysis results are sensitive to the selection of the control node and selection of lateral load pattern. In general, the centre of mass location at the roof of the building is considered as control node. For selecting lateral load pattern in pushover analysis, a set of guidelines as per FEMA 356 is explained in Section 2.4.2. The lateral load generally applied in both positive and negative directions in combination with gravity load (dead load and a portion of live load) to study the actual behaviour.

2.4.2 Lateral Load Profile

In pushover analysis the building is pushed with a specific load distribution pattern along the height of the building. The magnitude of the total force is increased but the pattern of the loading remains same till the end of the process. Pushover analysis results (*i.e.*, pushover curve, sequence of member yielding, building capacity and seismic demand) are very sensitive to the load pattern. The lateral load patterns should approximate the inertial forces expected in the building during an earthquake. The distribution of lateral inertial forces determines relative magnitudes of shears, moments, and deformations within the structure. The distribution of these forces will vary continuously during earthquake response as the members yield and stiffness characteristics change. It also depends on the type and magnitude of earthquake ground motion. Although the inertia force distributions vary with the severity of the earthquake and with time, FEMA 356 recommends primarily invariant load pattern for pushover analysis of framed buildings.

Several investigations (Mwafy and Elnashai, 2000; Gupta and Kunnath, 2000) have found that a triangular or trapezoidal shape of lateral load provide a better fit to dynamic analysis results at the elastic range but at large deformations the dynamic envelopes are closer to the uniformly distributed force pattern. Since the constant distribution methods are incapable of capturing such variations in characteristics of the structural behaviour under earthquake loading, FEMA 356 suggests the use of at least two different patterns for all pushover analysis. Use of two lateral load patterns is intended to bind the range that may occur during actual dynamic response. FEMA 356 recommends selecting one load pattern from each of the following two groups:

1. Group – I:

i) Code-based vertical distribution of lateral forces used in equivalent static analysis (permitted only when more than 75% of the total mass participates in the fundamental mode in the direction under consideration).

ii) A vertical distribution proportional to the shape of the fundamental mode in the direction under consideration (permitted only when more than 75% of the total mass participates in this mode).

iii) A vertical distribution proportional to the story shear distribution calculated by combining modal responses from a response spectrum analysis of the building (sufficient number of modes to capture at least 90% of the total building mass required to be considered). This distribution shall be used when the period of the fundamental mode exceeds 1.0 second.

2. Group – II:

i) A uniform distribution consisting of lateral forces at each level proportional to the total mass at each level.

ii) An adaptive load distribution that changes as the structure is displaced. The adaptive load distribution shall be modified from the original load distribution using a procedure that considers the properties of the yielded structure.

Instead of using the uniform distribution to bind the solution, FEMA 356 also allows adaptive lateral load patterns to be used but it does not elaborate the procedure. Although adaptive

procedure may yield results that are more consistent with the characteristics of the building under consideration it requires considerably more analysis effort. Fig. 2.4 shows the common lateral load pattern used in pushover analysis.

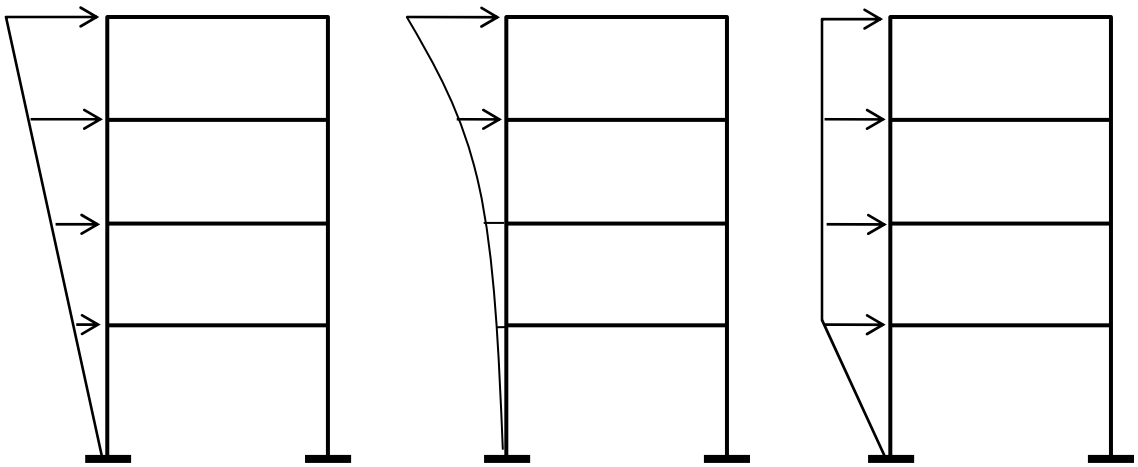

(a) Triangular (b) IS Code Based (c) Uniform

Fig. 2.4: Lateral load pattern for pushover analysis as per FEMA 356 (considering uniform mass distribution)

2.4.3 Target Displacement

Target displacement is the displacement demand for the building at the control node subjected to the ground motion under consideration. This is a very important parameter in pushover analysis because the global and component responses (forces and displacement) of the building at the target displacement are compared with the desired performance limit state to know the building performance. So the success of a pushover analysis largely depends on the accuracy of target displacement.

There are two approaches to calculate target displacement:

(a) Displacement Coefficient Method (DCM) and

(b) Capacity Spectrum Method (CSM).

Both of these approaches use pushover curve to calculate global displacement demand on the building from the response of an equivalent single-degree-of-freedom (SDOF) system. The only difference in these two methods is the technique used.

Displacement Coefficient Method

This method primarily estimates the elastic displacement of an equivalent SDOF system assuming initial linear properties and damping for the ground motion excitation under consideration. Then it estimates the total maximum inelastic displacement response for the building at roof by multiplying with a set of displacement coefficients.

The process begins with the base shear versus roof displacement curve (pushover curve) as shown in Fig. 2.5a. An equivalent period (T_{eq}) is generated from initial period (T_i) by graphical procedure. This equivalent period represents the linear stiffness of the equivalent SDOF system. The peak elastic spectral displacement corresponding to this period is calculated directly from the response spectrum representing the seismic ground motion under consideration (Fig. 2.5b).

$$S_d = \frac{T_{eq}^2}{4\pi^2} S_a \tag{2.7}$$

Now, the expected maximum roof displacement of the building (target displacement) under the selected seismic ground motion can be expressed as:

$$\delta_t = C_0 C_1 C_2 S_d = C_0 C_1 C_2 \frac{T_{eq}^2}{4\pi^2} S_a \tag{2.8}$$

Where,

C_0 = a shape factor (often taken as the first mode participation factor) to convert the spectral displacement of equivalent SDOF system to the displacement at the roof of the building.

C_1 = the ratio of expected displacement (elastic plus inelastic) for an inelastic system to the displacement of a linear system.

C_2 = a factor that accounts for the effect of pinching in load deformation relationship due to strength and stiffness degradation

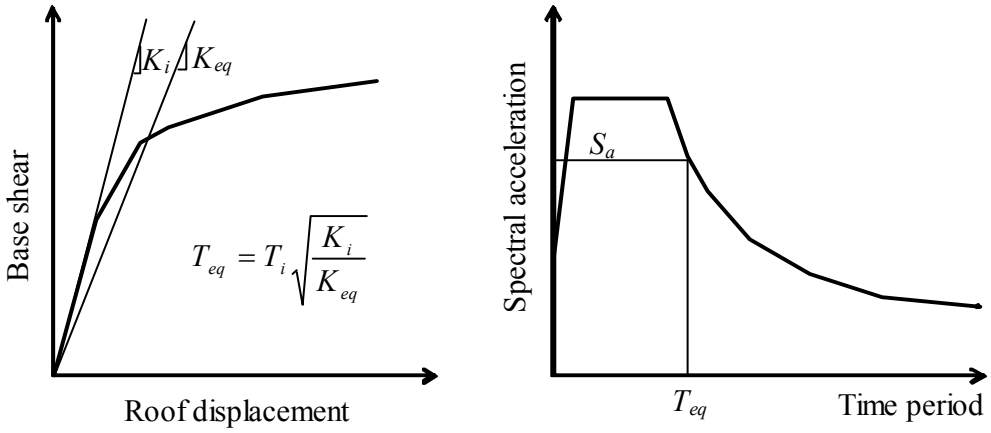

(a) Pushover Curve (b) Elastic Response Spectrum

Fig. 2.5: Schematic representation of Displacement Coefficient Method (ASCE/SEI 41-06)

Table 2.1: Values of C_0 factor for shear building as per ASCE/SEI 41-06

Number of storeys	Shear Building		Other building
	Triangular Load Pattern	Uniform Load Pattern	
1	1.0	1.00	1.00
2	1.2	1.15	1.20
3	1.2	1.20	1.30
5	1.3	1.20	1.40
10+	1.3	1.20	1.50

These coefficients are derived empirically from statistical studies of the nonlinear response history analyses of SDOF systems of varying periods and strengths and given in ASCE/SEI 41-06. As per ASCE/SEI 41-06, the values of C_0 factor for shear buildings depends on the number of storeys and the lateral load pattern used in the pushover analysis. Table 2.1 presents the values of C_0 provided by the ASCE/SEI 41-06 for shear buildings.

Capacity Spectrum Method (ATC-40)

The basic assumption in Capacity Spectrum Method is also the same as the previous one. That is, the maximum inelastic deformation of a nonlinear SDOF system can be approximated from the maximum deformation of a linear elastic SDOF system with an equivalent period and damping. This procedure uses the estimates of ductility to calculate effective period and damping. This procedure uses the pushover curve in an acceleration-displacement response spectrum (ADRS) format. This can be obtained through simple conversion using the dynamic properties of the system. The pushover curve in an ADRS format is termed a 'capacity spectrum' for the structure. The seismic ground motion is represented by a response spectrum in the same ADRS format and it is termed as demand spectrum (Fig. 2.6).

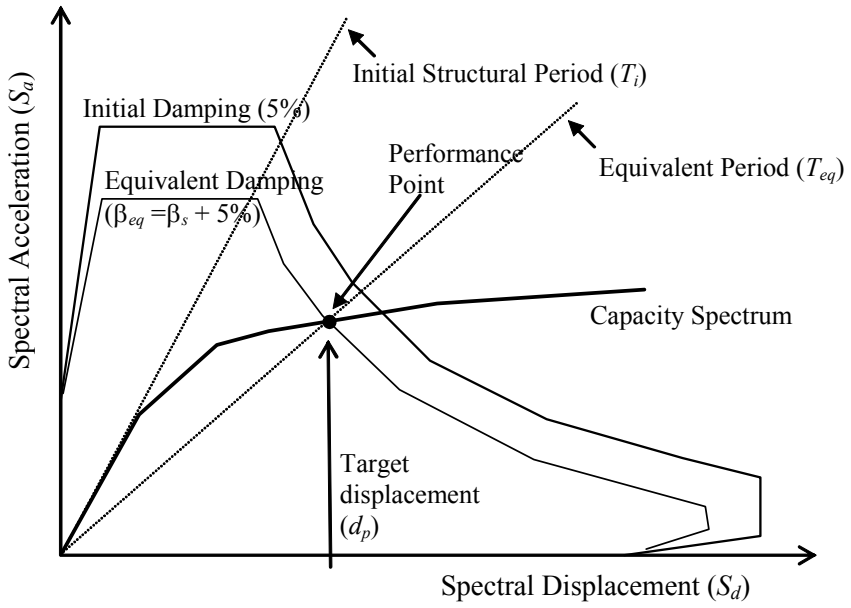

Fig. 2.6: Schematic representation of Capacity Spectrum Method (ATC 40)

The equivalent period (T_{eq}) is computed from the initial period of vibration (T_i) of the nonlinear system and displacement ductility ratio (μ). Similarly, the equivalent damping ratio (β_{eq}) is computed from initial damping ratio (ATC 40 suggests an initial elastic viscous damping ratio of 0.05 for reinforced concrete building) and the displacement ductility ratio (μ). ATC 40 provides the following equations to calculate equivalent time period (T_{eq}) and equivalent damping (β_{eq}).

$$T_{eq} = T_i \sqrt{\frac{\mu}{1 + \alpha\mu - \alpha}} \tag{2.9}$$

$$\beta_{eq} = \beta_i + \kappa \frac{2}{\pi} \frac{(\mu - 1)(1 - \alpha)}{\mu(1 + \alpha\mu - \alpha)} = 0.05 + \kappa \frac{2}{\pi} \frac{(\mu - 1)(1 - \alpha)}{\mu(1 + \alpha\mu - \alpha)} \tag{2.10}$$

where α is the post-yield stiffness ratio and κ is an adjustment factor to approximately account for changes in hysteretic behaviour in reinforced concrete structures.

ATC 40 relates effective damping to the hysteresis curve (Fig. 2.7) and proposes three hysteretic behaviour types that alter the equivalent damping level. Type A hysteretic behaviour is meant for new structures with reasonably full hysteretic loops, and the corresponding equivalent damping ratios take the maximum values. Type C hysteretic behaviour represents severely degraded hysteretic loops, resulting in the smallest equivalent damping ratios. Type B hysteretic behaviour is an intermediate hysteretic behaviour between types A and C. The value of κ decreases for degrading systems (hysteretic behaviour types B and C).

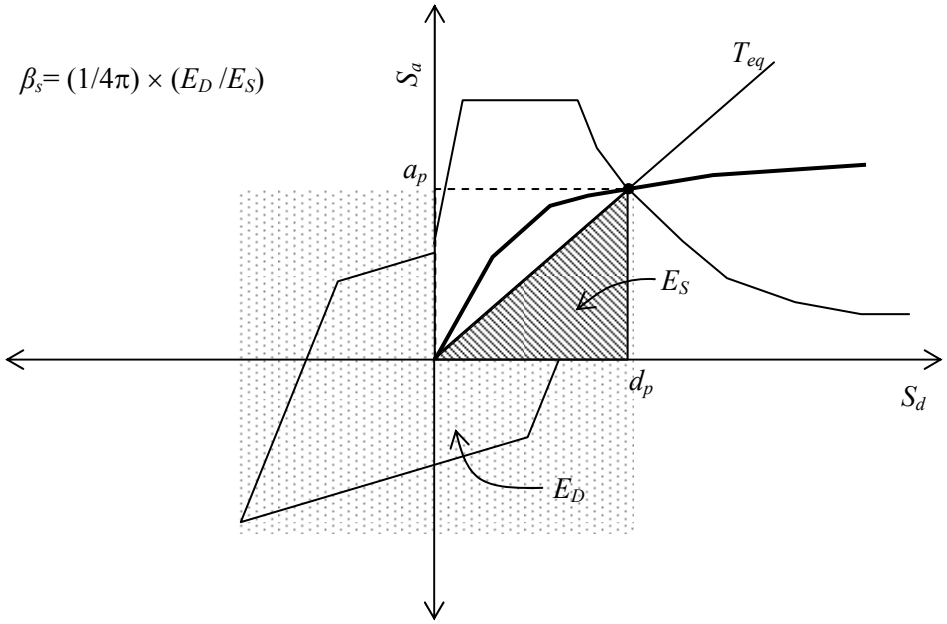

Fig. 2.7: Effective damping in Capacity Spectrum Method (ATC 40)

The equivalent period in Eq. 2.9 is based on a lateral stiffness of the equivalent system that is equal to the secant stiffness at the target displacement. This equation does not depend on the

degrading characteristics of the hysteretic behaviour of the system. It only depends on the displacement ductility ratio (μ) and the post-yield stiffness ratio (α) of the inelastic system.

ATC 40 provides reduction factors to reduce spectral ordinates in the constant acceleration region and constant velocity region as a function of the effective damping ratio. The spectral reduction factors are given by:

$$SR_A = \frac{3.21 - 0.68\ln(100\beta_{eq})}{2.12} \tag{2.11}$$

$$SR_V = \frac{2.31 - 0.41\ln(100\beta_{eq})}{1.65} \tag{2.12}$$

where β_{eq} is the equivalent damping ratio, SR_A is the spectral reduction factor to be applied to the constant acceleration region, and SR_V is the spectral reduction factor to be applied to the constant velocity region (descending branch) in the linear elastic spectrum.

Since the equivalent period and equivalent damping are both functions of the displacement ductility ratio (Eq. 2.9 and Eq. 2.10), it is required to have prior knowledge of displacement ductility ratio. However, this is not known at the time of evaluating a structure. Therefore, iteration is required to determine target displacement. ATC 40 describes three iterative procedures with different merits and demerits to reach the solution.

2.5 SUMMARY

This chapter begins with a brief literature review on the seismic behaviour of URM buildings. The literature review found that only a little research effort has been devoted in to the nonlinear

analysis of URM building. However, a number of design manuals (ASCE/SEI 41, FEMA-440, FEMA-356, etc.) have stated the importance of nonlinear analysis in the seismic evaluation and retrofit of existing URM buildings. The guideline for nonlinear static analysis given in ASCE/SEI 41 is the most recent among others. The modelling of nonlinear force-drift relation is an important parameter for carrying out the nonlinear static (pushover) analysis. The properties of bricks vary from kiln to kiln as it is very difficult to control the properties of constituents and their mix proportions. Therefore, modelling nonlinear force-drift relation for URM masonry wall should be established for Indian construction practice. Also, carrying out nonlinear analysis is found to be difficult for analyse two-dimensional wall elements. There are few approach proposed in literature to idealised the URM wall segments as an equivalent frame elements for this purpose. Critical reviews on these methods are essential to get better clarity.

Also, this chapter presents a brief overview of the pushover analysis method as given in ASCE/SEI 41-06.

CHAPTER 3

LATERAL LOAD RESISTING BEHAVIOUR OF MASONRY WALL

3.1 INTRODUCTION

An experimental program has been carried out as part of this research to study the behaviour of URM wall panels under monotonic lateral loading. This chapter begins with the details of experimental setup, description of the test specimens and the results obtained from the experimental investigations.

Second part of this chapter present an evaluation of existing pushover analysis method (ASCE/SEI 41-06) for URM building based on the results of the experimental studies. This chapter finally presents a set of modification to the ASCE/SEI 41-06 method of pushover analysis for improved results.

3.2 TEST SPECIMENS

Sixteen wall panels of varying dimensions were tested for in-plane monotonic lateral loads. For each specimen the axial compressive load was maintained as a constant during testing. A window opening at prescribed location of the test specimen was provided for eight of the sixteen specimens and its in-plane monotonic lateral load behaviour was studied. Four additional specimens with a door opening in combination with a window opening were tested for their in-plane monotonic lateral load behaviour. Four solid walls

without any opening were also tested and compared with the behaviour of similar panels with openings.

Details of the test specimens are shown in the Table 3.1. The objective was to study the effect of the presence of opening on the panel behaviour, when subjected to monotonic lateral loading. In the table, ‘S’ stands for Solid Wall specimen whereas ‘W’ and ‘D’ denotes for the window and door opening respectively. Location for the opening in the specimen is defined by the parameters c, d, and e as shown in the Fig. 3.1. Sizes of the window opening are defined by the width (a) and height (b) and this for door opening is defined by Width (w) and height (h).

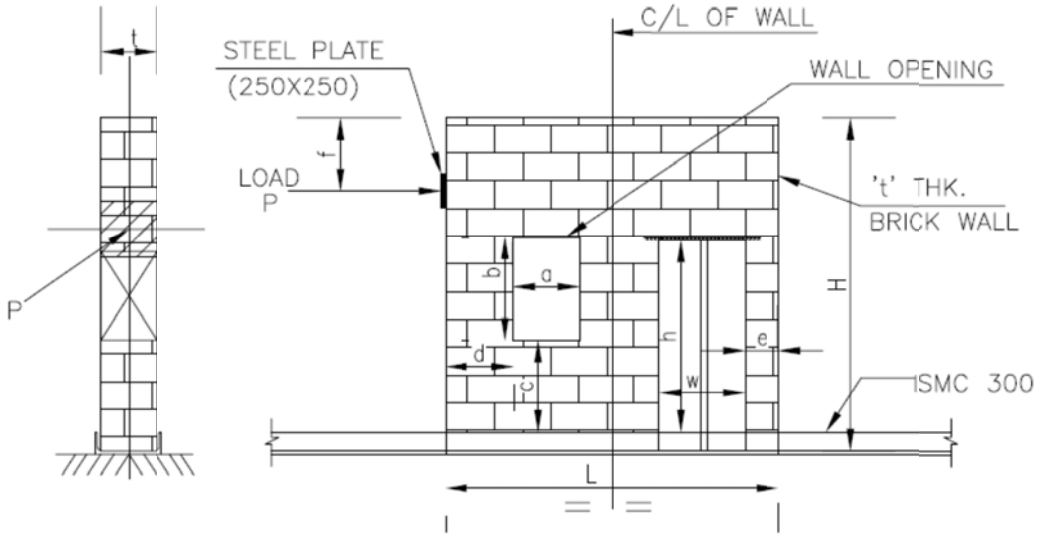

Fig. 3.1: Details of a typical sample

Table 3.1: Details of test specimens for lateral loading

Specimen ID	Opening	Length, L (m)	Height, H (m)	Thickness, t (m)	Window Opening				Door Opening		
					Width, a (m)	Height, b (m)	Location, c (m)	Location, d (m)	Width, w (m)	Height, h (m)	Location, e (m)
W-S1	S	1.5	2.25	0.250	-	-	-	-	-	-	-
W-S2	S	2.0	0.80	0.250	-	-	-	-	-	-	-
W-S3	S	1.5	2.25	0.125	-	-	-	-	-	-	-
W-S4	S	2.0	0.80	0.125	-	-	-	-	-	-	-
W-01	W	1.5	1.50	0.250	0.260	0.540	0.410	0.30	-	-	-
W-02	W	1.5	2.25	0.250	0.260	0.820	0.615	0.30	-	-	-
W-03	W	2.0	1.50	0.250	0.235	0.430	0.330	0.33	-	-	-
W-04	W	2.0	0.80	0.250	0.345	0.290	0.220	0.63	-	-	-
W-05	W	1.5	1.50	0.125	0.360	0.545	0.410	0.30	-	-	-
W-06	W	1.5	2.25	0.125	0.350	0.560	0.320	0.40	-	-	-
W-07	W	2.0	1.50	0.125	0.235	0.430	0.330	0.85	-	-	-
W-08	W	2.0	0.80	0.125	0.345	0.290	0.220	0.63	-	-	-
W-09	D & W	1.5	1.50	0.250	0.240	0.525	0.410	0.30	0.380	0.975	0.33
W-10	D & W	1.5	2.25	0.250	0.255	0.850	0.615	0.35	0.385	1.430	0.33
W-11	D & W	2.0	1.50	0.250	0.235	0.430	0.330	0.60	0.250	0.460	0.24
W-12	D & W	2.0	0.80	0.250	0.330	0.260	0.220	0.63	0.515	0.510	0.50

3.3 TEST SET-UP

Each wall panels were placed on a 300mm thick foundation. An ISMC 300 channel attached rigidly with the foundation was connected with the strong floor of the laboratory to transfer the load to the ground and a fixed support condition is achieved as shown in Fig. 3.2. Burnt clay brick of 230×110×70 mm sizes were used with cement-sand mortar of 1:5 proportion to make the wall specimens. Average compressive strength of the unit brick was found to be 13 MPa after 28 days of curing. Average compressive strength of cement-sand mortar was found to be 6.3 MPa after 28 days of curing. Three mild steel bars of 10 mm diameter were provided at the top of door and window opening to transfer the load.

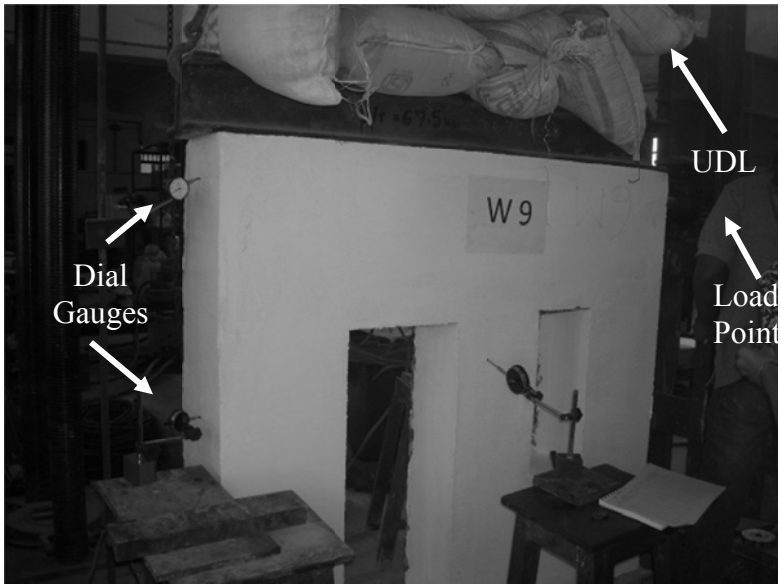

Fig. 3.2(a): Test setup for Wall Sample# W9

Sand bags of required weight were used uniformly to apply constant axial load at the top of each test specimens. In-plane monotonic lateral loads were applied to the test specimens by hydraulic load cell attached to the vertical rigid wall as shown in Figs. 3.2(a)-3.2(c).

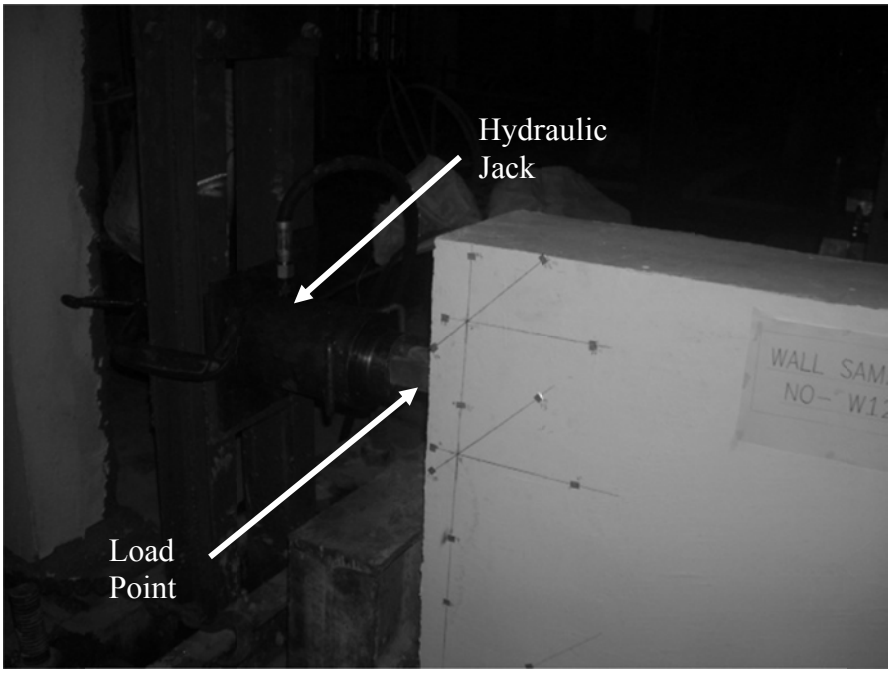

Fig. 3.2(b): Test setup for Wall Sample no W12

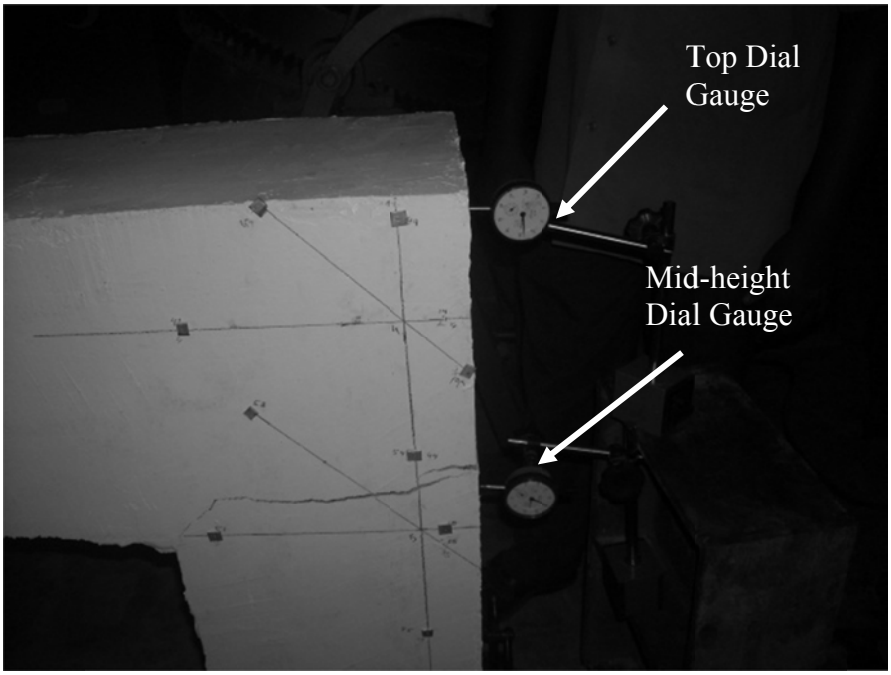

Fig. 3.2(c): Test setup for Wall Sample no W11

3.4 RESULTS OF IN-PLANE MONOTONIC LATERAL LOAD TEST

This section presents the results obtained from the experimental study on the sixteen unreinforced masonry wall specimens with and without opening for in-plane monotonic lateral load. Figs. 3.3-3.18 present the load deformation behaviour of the sixteen wall panels. Displacements were measured at two points: one at the top of the wall and the other at the mid-height. These figures show that, in most of the cases, the displacement at the mid height of the wall is more than half the top wall displacement. This indicates that there is a change in slope in at the mid-height of the wall. This may be due to the presence of opening at the mid height which is initiating failure.

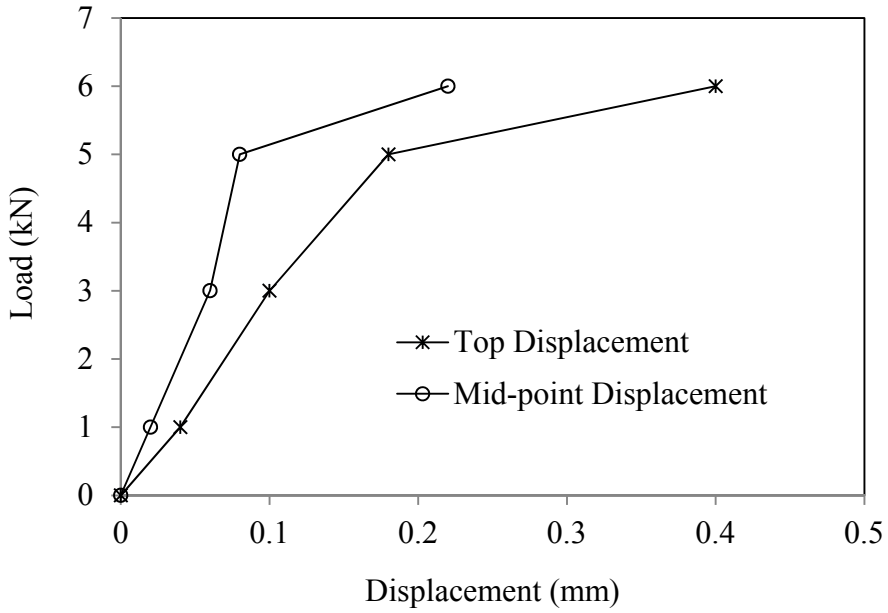

Fig. 3.3 Load-displacement relation obtained from experiment for Wall Panel W-S1

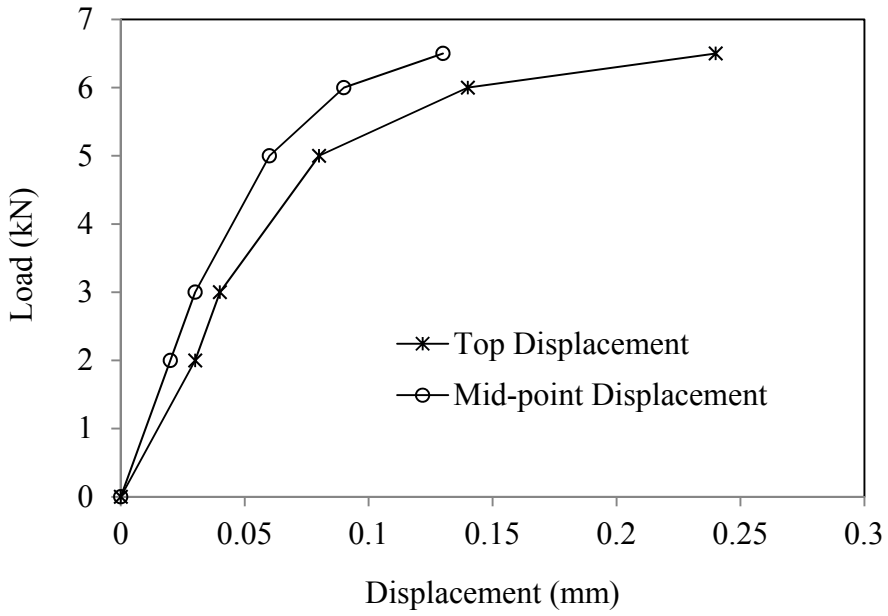

Fig. 3.4 Load-displacement relation obtained from experiment for Wall Panel W-S2

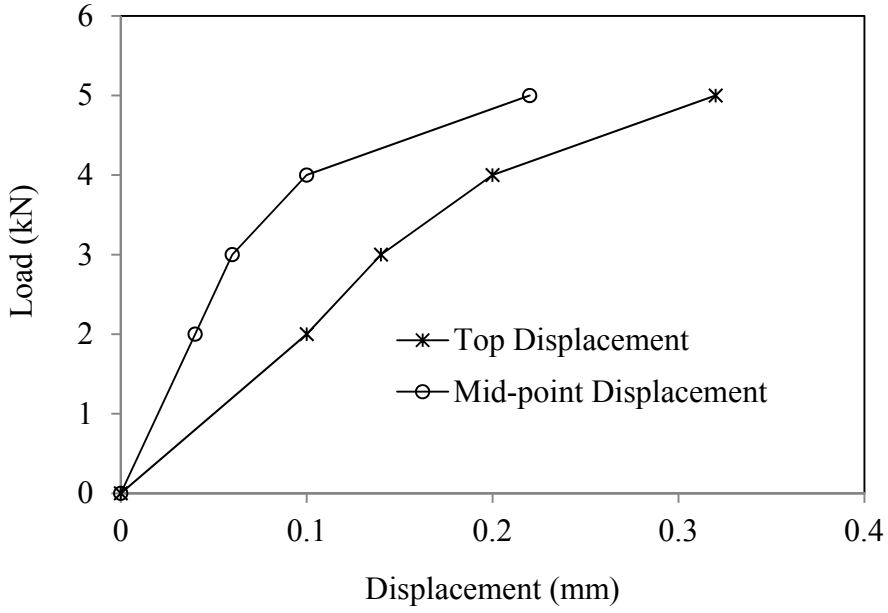

Fig. 3.5 Load-displacement relation obtained from experiment for Wall Panel W-S3

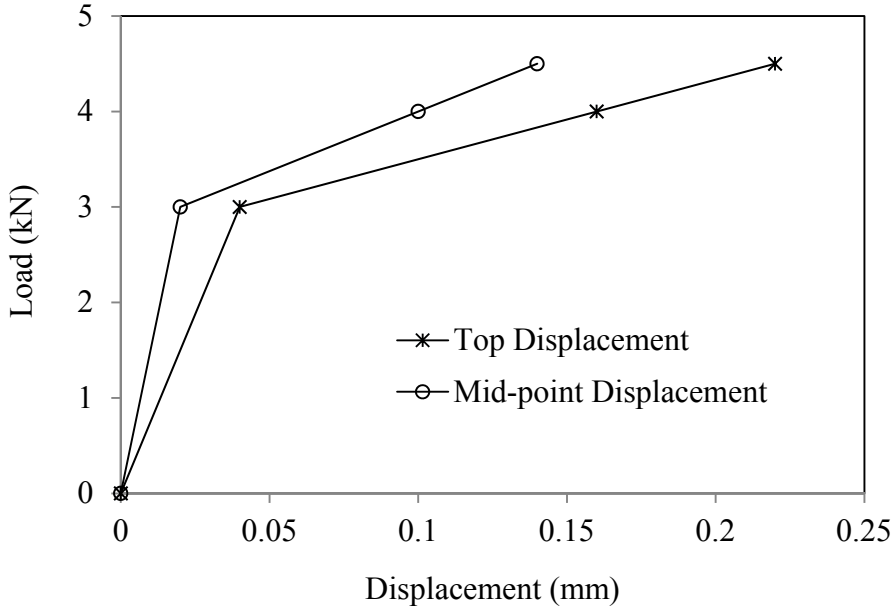

Fig. 3.6 Load-displacement relation obtained from experiment for Wall Panel W-S4

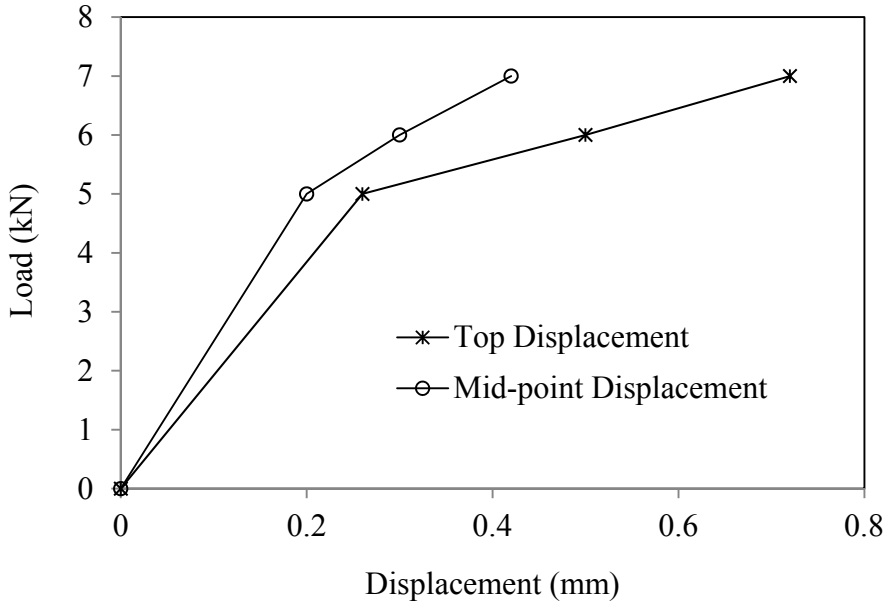

Fig. 3.7 Load-displacement relation obtained from experiment for Wall Panel W1

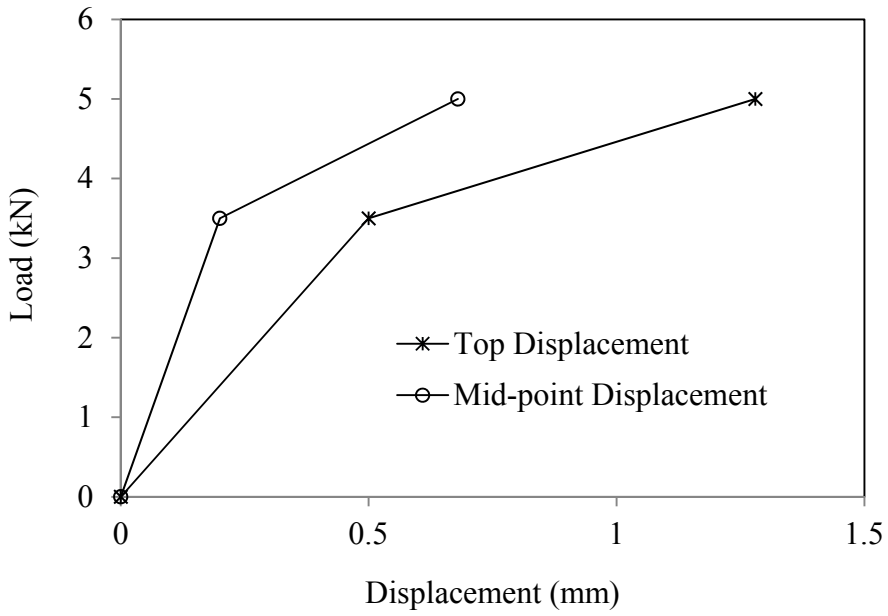

Fig. 3.8 Load-displacement relation obtained from experiment for Wall Panel W2

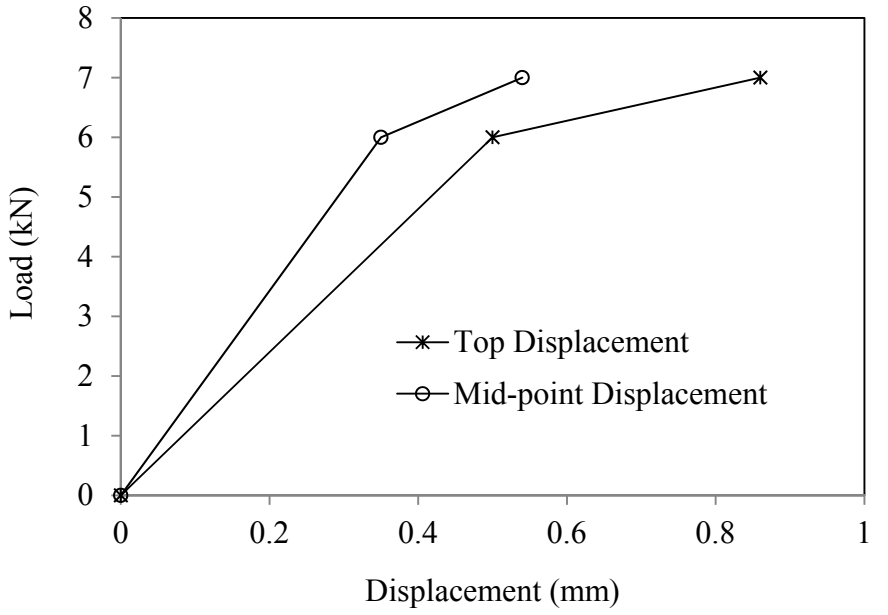

Fig. 3.9 Load-displacement relation obtained from experiment for Wall Panel W3

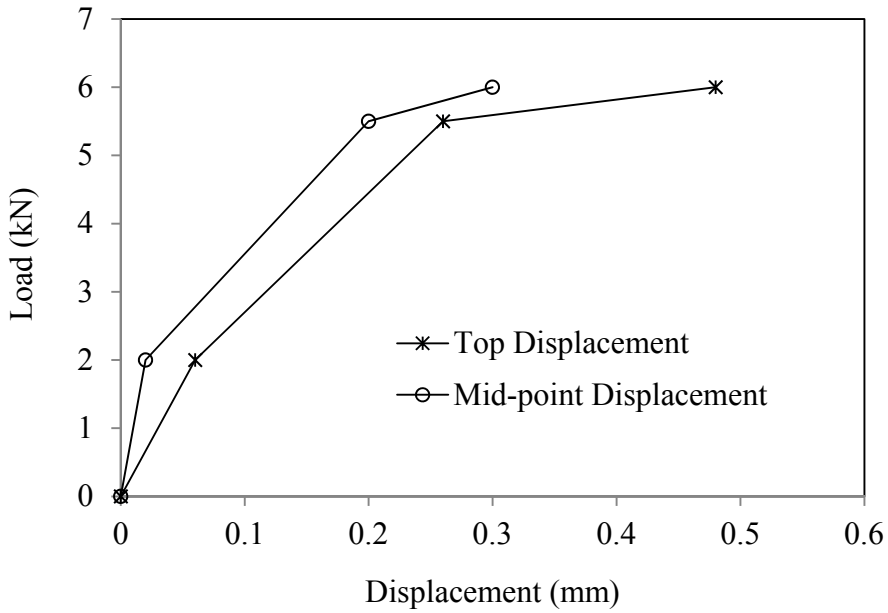

Fig. 3.10 Load-displacement relation obtained from experiment for Wall Panel W4

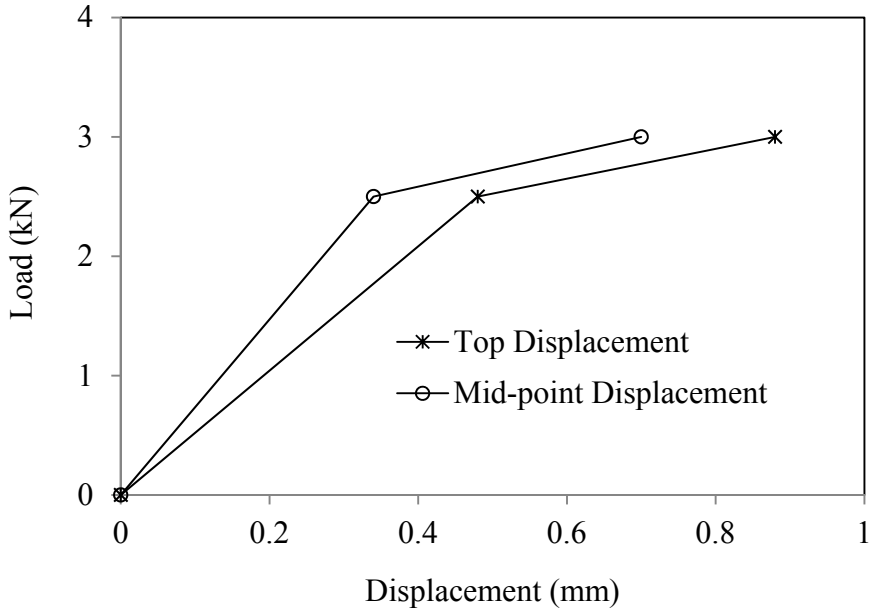

Fig. 3.11 Load-displacement relation obtained from experiment for Wall Panel W5

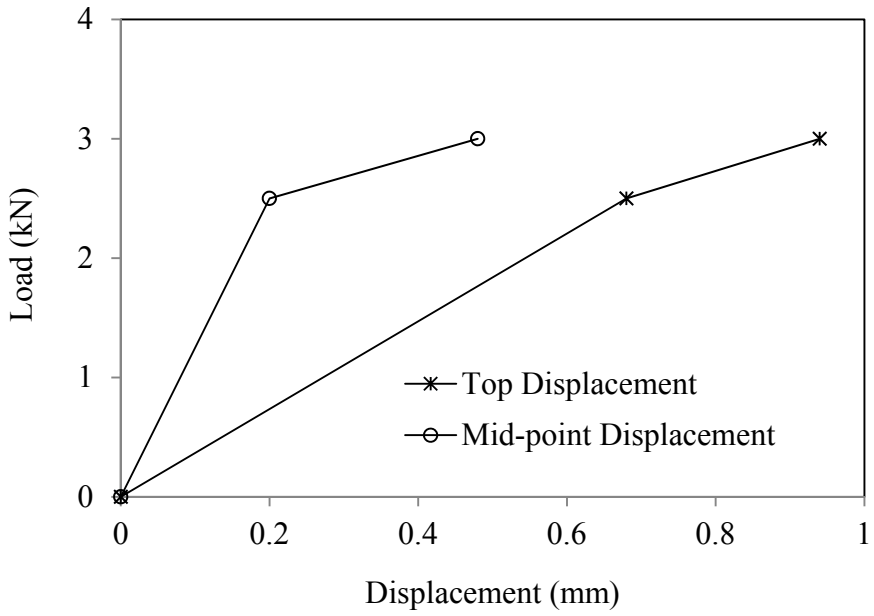

Fig. 3.12 Load-displacement relation obtained from experiment for Wall Panel W6

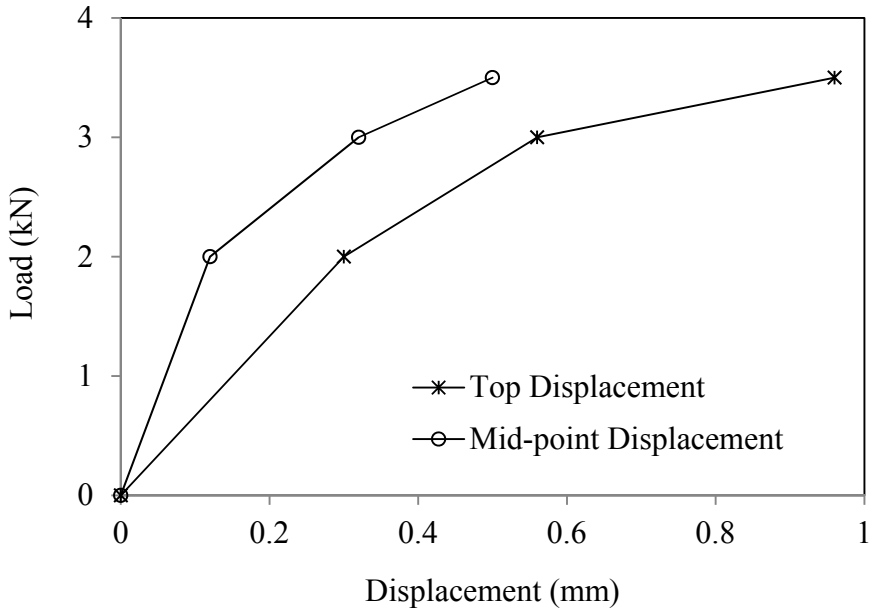

Fig. 3.13 Load-displacement relation obtained from experiment for Wall Panel W7

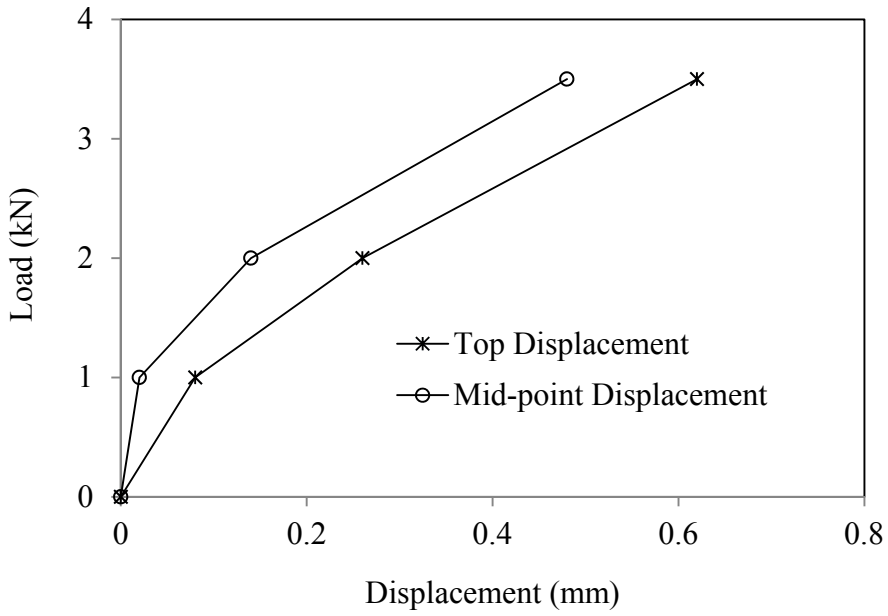

Fig. 3.14 Load-displacement relation obtained from experiment for Wall Panel W8

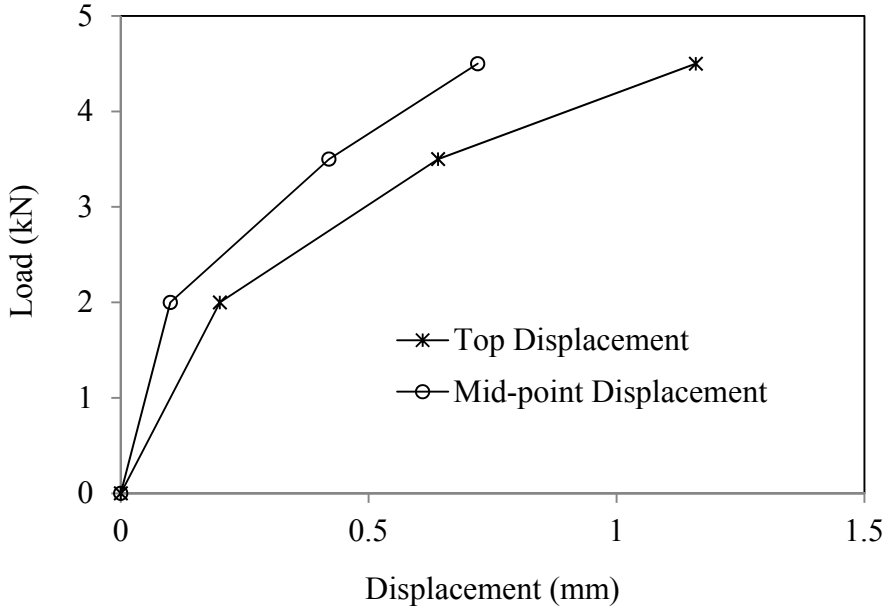

Fig. 3.15 Load-displacement relation obtained from experiment for Wall Panel W9

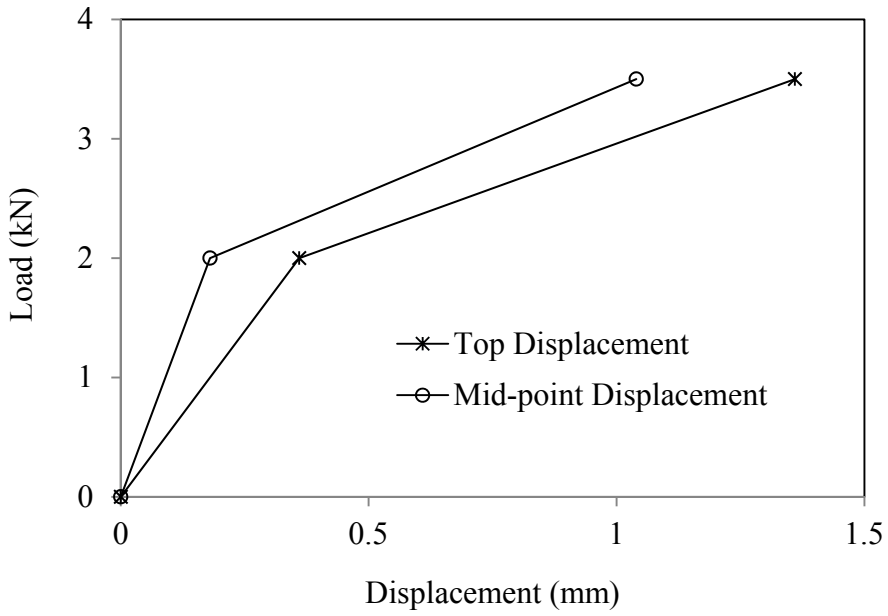

Fig. 3.16 Load-displacement relation obtained from experiment for Wall Panel W10

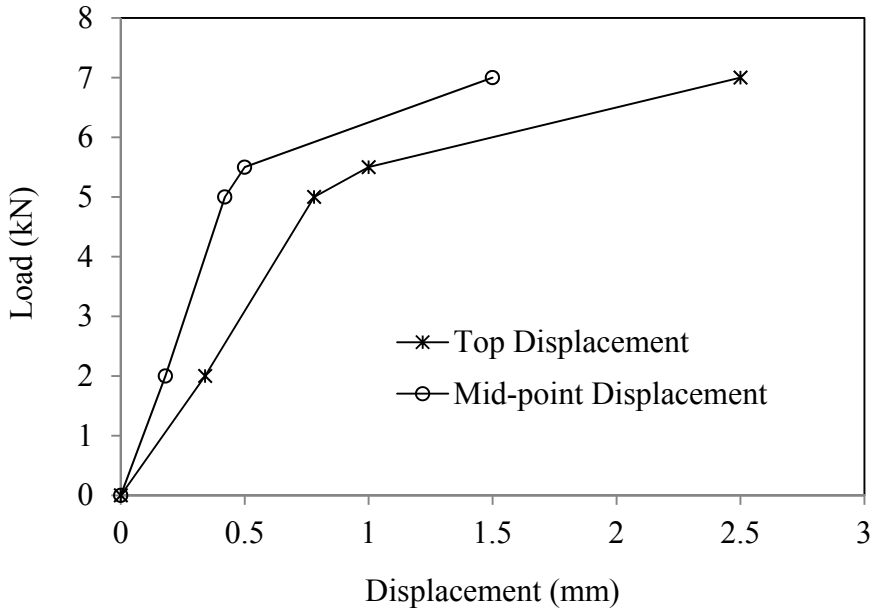

Fig. 3.17 Load-displacement relation obtained from experiment for Wall Panel W11

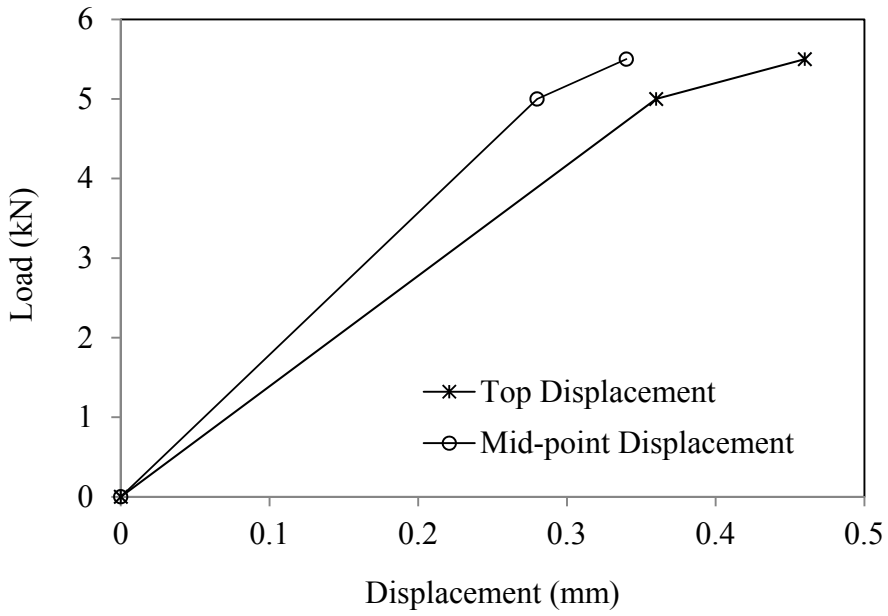

Fig. 3.18 Load-displacement relation obtained from experiment for Wall Panel W12

The experimental results presented above are tabulated in Table 3.2. This table also compare the experimental results with the ASCE/SEI 41-06 recommendations. This is to be noted that the ASCE/SEI 41-06 recommendations are for the solid walls whereas the experimental results presented here are for both solid walls and walls with openings.

Table 3.2: Comparison of the experimental results and ASCE/SEI 41-06 recommendations

Specimen ID	A_v (m^2)	I_g (m^4)	P_D (kN)	ASCE/SEI 41-06 (Solid)		Experimental						
				K (kN/m) $\times 10^4$	Q_{CE} (kN)	K_e (kN/m) $\times 10^4$	αK_e (kN/m)	Q_y (kN)	Q_{ult} (kN)	Δ_y (mm)	Δ_{ult} (mm)	%H
W-S1	0.375	0.0703	5.63	7.34	2.53	2.78	4545	5.0	6.0	0.18	0.40	0.018
W-S2	0.500	0.1667	2.65	52.80	4.46	4.29	5000	6.0	6.5	0.14	0.24	0.030
W-S3	0.188	0.0352	2.81	3.67	1.27	2.00	8333	4.0	5.0	0.20	0.32	0.014
W-S4	0.250	0.0833	1.33	26.40	2.23	2.50	8333	4.0	4.5	0.16	0.22	0.028
W-01	0.310	0.0633	3.75	13.10	2.53	1.20	4545	6.0	7.0	0.50	0.72	0.048
W-02	0.310	0.0633	5.63	6.33	2.53	0.70	1923	3.5	5.0	0.50	1.28	0.057
W-03	0.441	0.1485	5.00	21.20	4.50	1.20	2778	6.0	7.0	0.50	0.86	0.057
W-04	0.414	0.1624	2.65	44.20	4.46	2.12	2273	5.5	6.0	0.26	0.48	0.060
W-05	0.143	0.0314	1.88	6.16	1.27	0.52	1250	2.5	3.0	0.48	0.88	0.059
W-06	0.144	0.0334	2.81	3.12	1.27	0.37	1923	2.5	3.0	0.68	0.94	0.042
W-07	0.221	0.0832	2.50	10.80	2.25	0.57	1250	3.0	3.5	0.56	0.96	0.064
W-08	0.207	0.0812	1.33	22.10	2.23	0.77	4167	2.0	3.5	0.26	0.62	0.078
W-09	0.220	0.0573	8.35	9.95	5.64	0.55	1923	3.5	4.5	0.64	1.16	0.077
W-10	0.215	0.0591	9.03	5.03	4.06	0.56	1500	2.0	3.5	0.36	1.36	0.060
W-11	0.379	0.1362	5.00	18.40	4.50	0.64	1163	5.0	7.0	0.78	2.50	0.167
W-12	0.289	0.1520	2.65	31.30	4.46	1.39	5000	5.0	5.5	0.36	0.46	0.058

Fig. 3.19 Typical crack pattern of the test specimen (W-10)

3.4.1 Effect of Opening

Fig. 3.20 presents load deformation behaviour of three walls with identical thickness (250 mm) and aspect ratio (height to length ratio is equals to 0.40) with different openings. This figure shows that the introduction of opening in an URM wall reduces the stiffness significantly. However, the reduction of strength is found to be marginal. It is to be noted

that the wall W12 has tested under a greater axial force than other two walls presented in this figure which is responsible for the higher ultimate load capacity of wall W12.

Figs. 3.21-3.23 present the similar observations for walls with other different aspect ratios (0.75, 1.00, and 1.50) and constant thickness of 250 mm.

Figs. 3.24-3.25 presents the similar results for thinner walls (thickness = 125 mm). This may be noted here that door openings were provided in the thicker (250 mm) walls only.

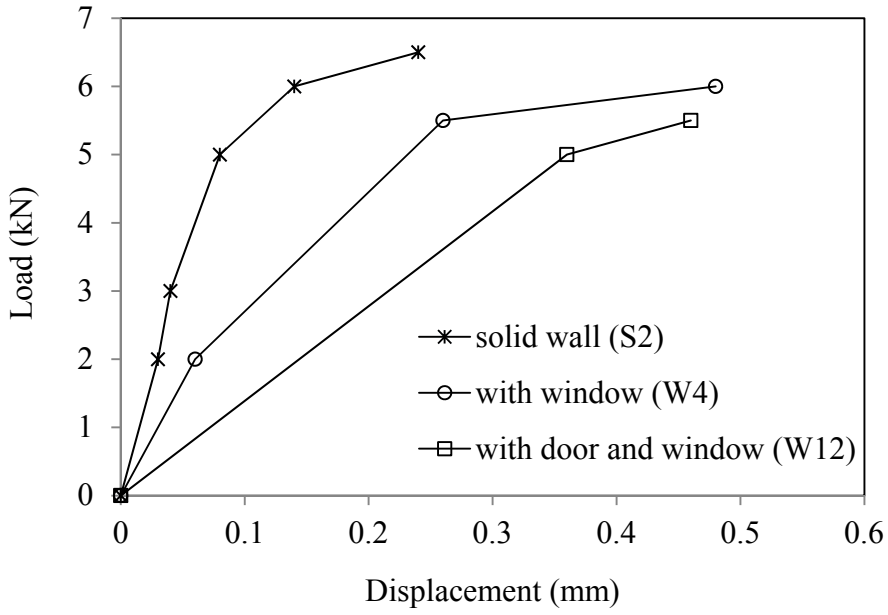

Fig. 3.20 Load-displacement relations of wall with constant thickness (250mm) and constant aspect ratio (h/L = 0.4)

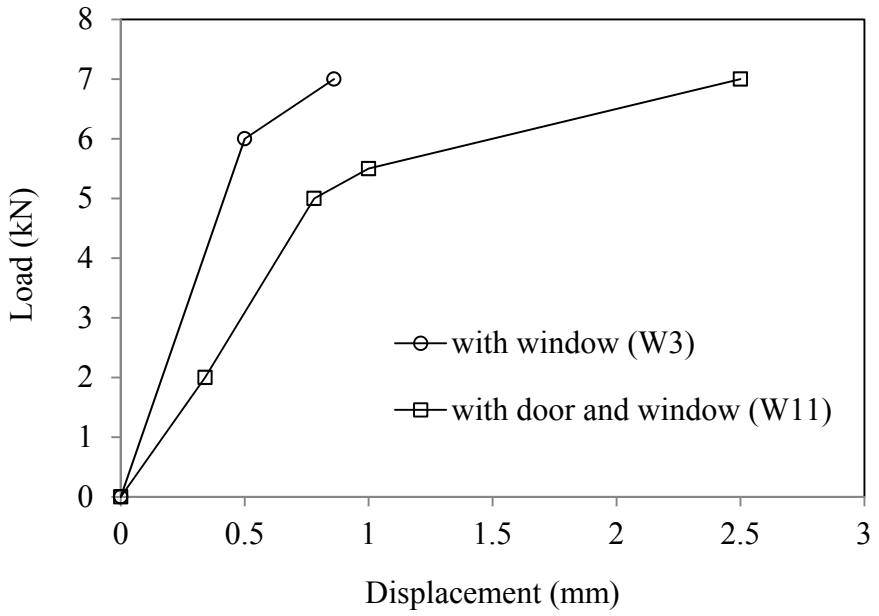

Fig. 3.21 Load-displacement relations of wall with constant thickness (250mm) and constant aspect ratio (h/L = 0.75)

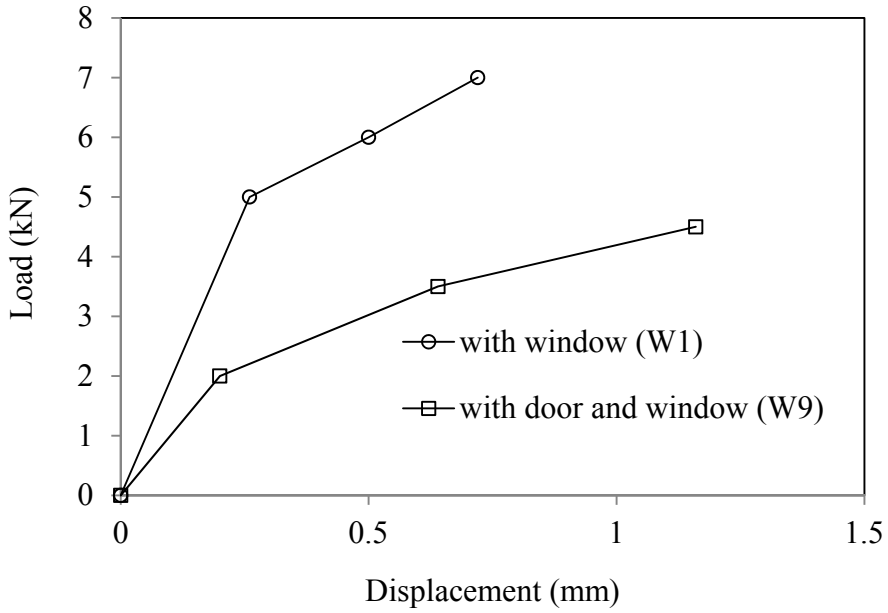

Fig. 3.22 Load-displacement relations of wall with constant thickness (250mm) and constant aspect ratio (h/L = 1.0)

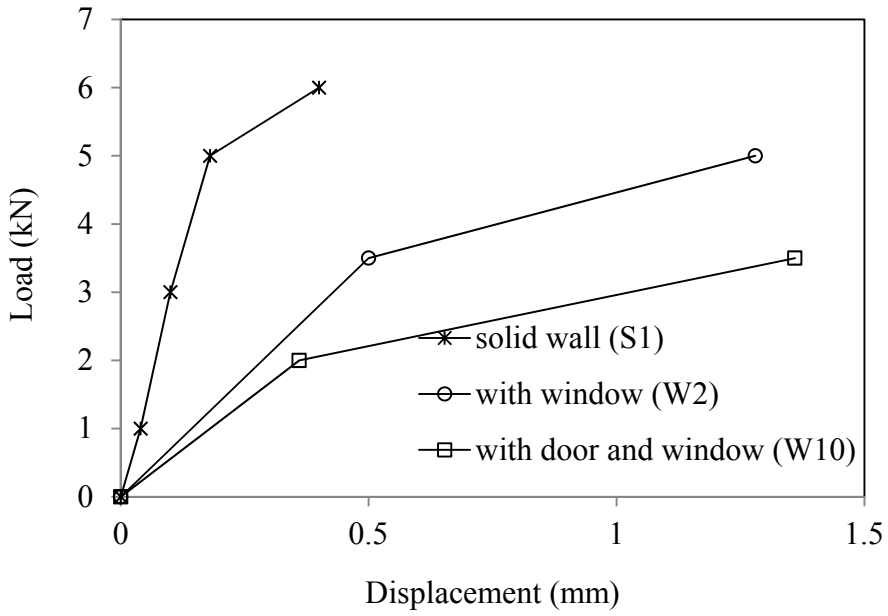

Fig. 3.23 Load-displacement relations of wall with constant thickness (250mm) and constant aspect ratio (h/L = 1.5)

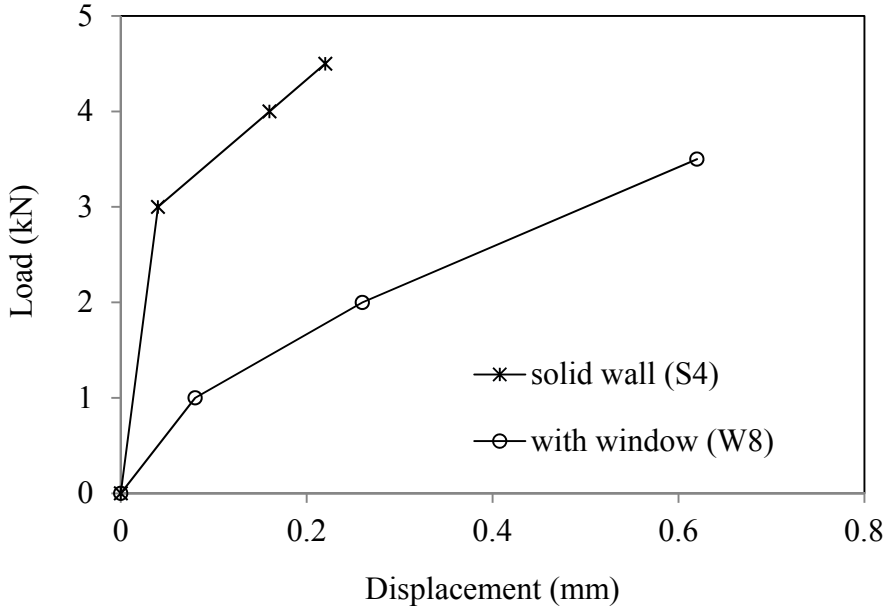

Fig. 3.24 Load-displacement relations of wall with constant thickness (125mm) and constant aspect ratio (h/L = 0.4)

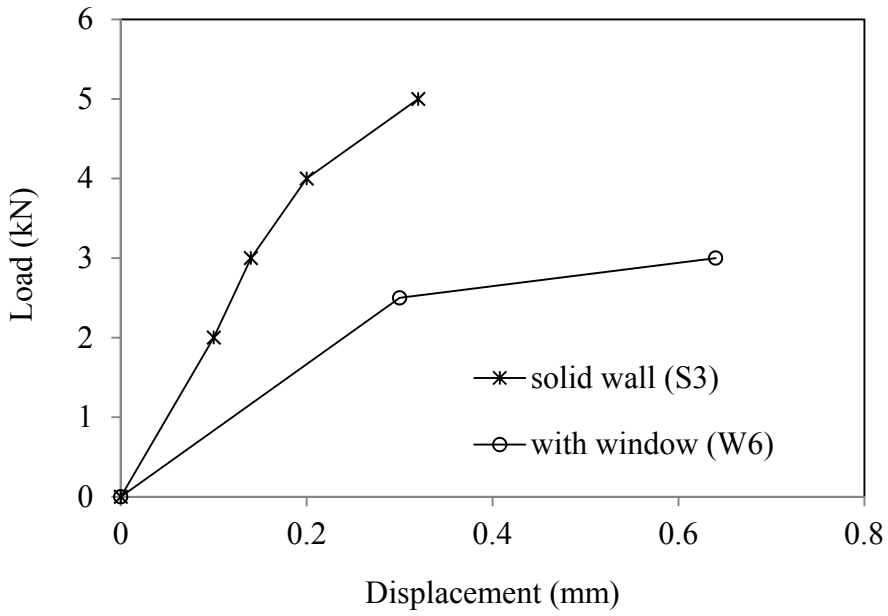

Fig. 3.25 Load-displacement relations of wall with constant thickness (125mm) and constant aspect ratio (h/L = 1.5)

3.4.2 Effect of Aspect Ratio

Figs. 3.26 and 3.27 show the load deformation behaviour for URM walls of constant thickness (250 mm and 125 mm respectively) with varying aspect ratios. The two figures are representing walls with different opening category. These figures show that the aspect ratio affects the stiffness of the wall significantly. However, the results presented here do not give any trend for the relation between strength of the wall and the wall aspect ratio. This is due to the fact that the sizes of door and window openings are not uniform for all the walls tested here.

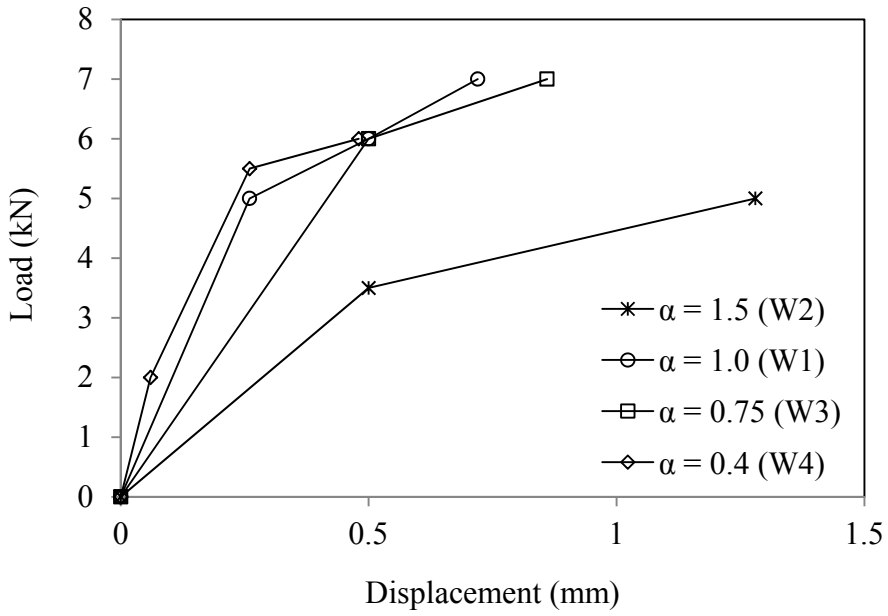

Fig. 3.26 Load-displacement relations of wall with constant thickness (250mm) and with only window opening

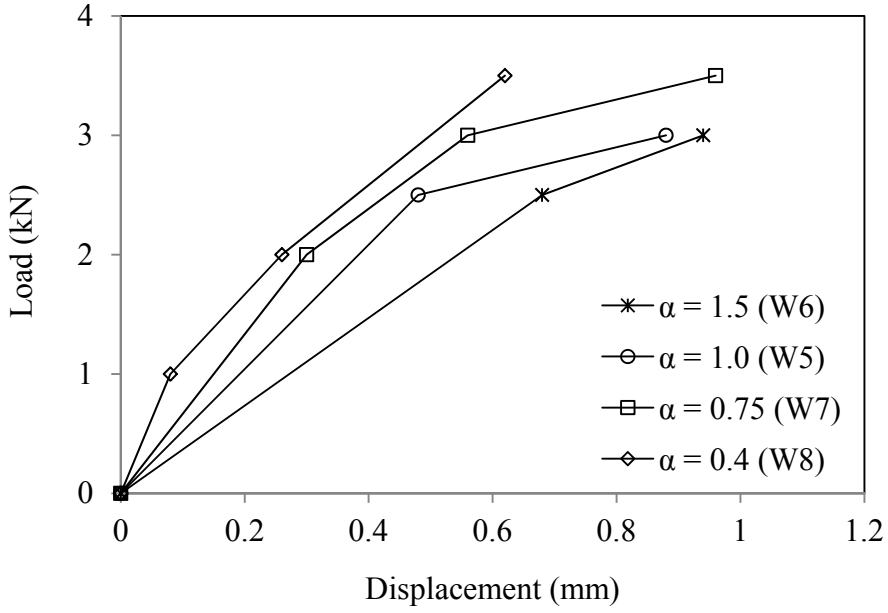

Fig. 3.27 Load-displacement relations of wall with constant thickness (125 mm) and with only window opening

3.5 ASSESSMENT OF LATERAL LOAD RESISTING BEHAVIOUR OF URM WALL

The objective of this section is to study the numerical procedure to assess the lateral load resisting behaviour of URM wall panel. It is important to create a mathematical model to analyse any structure. The model must ideally represent the mass distribution, strength, stiffness and deformability of actual wall panel. Modelling of the material properties and structural elements used in the present study is discussed in the following sub-sections. All the sixteen wall panels used in experimental study were modelled and analysed for nonlinear static (pushover analysis). The resulting base shear versus top displacement behaviour was compared with the experimental results.

3.5.1 Modelling for Linear Analysis

A three-dimensional linear elastic computer model of the building has been developed using the computer program SAP 2000. Walls are modelled using plate elements with orthotropic properties. Orthotropic material properties of the masonry wall were taken from Jurina and Peano (1982) and presented in Table 3.3. These values of elastic properties correspond to the brick-to-mortar Young's Modulus ratio is equal to three. Each wall panel is divided into small finite element meshes for convergence. Face wall and cross wall connected properly at the junction. For dynamic analyses, the mass of the slab was lumped at the centre of mass location at each floor level. This was located at the design eccentricity (based on IS 1893:2002) from the calculated centre of stiffness. Design lateral forces at each storey level were applied at the centre of mass locations independently in two horizontal directions.

Table 3.3: Material constants used for the orthotropic wall panel

E_b/E_m	E_1 (MPa)	E_2 (MPa)	E_3 (MPa)	G_{12} (MPa)	G_{23} (MPa)	G_{31} (MPa)	ν_{12}	ν_{23}	ν_{31}
3	4694	4464	4237	2344	1710	1942	0.144	0.139	0.130

End of the walls at the foundation were modelled as fixed support at the top of the foundation considering compacted hard soil above foundation. The structural effect of slabs due to their in-plane stiffness is taken into account by assigning 'diaphragm' action at each floor level. The mass/weight contribution of slab is modelled separately on the supporting walls. Staircase is not modelled for their stiffness but its mass was considered in the static and dynamic analyses. The design spectrum for medium soil specified in IS 1893:2002 was used for the analyses. The effect of soil-structure interaction was ignored in the analyses. The first 20 modes were considered for the dynamic analysis, which gives more than 80% mass participation in both the horizontal directions. The SRSS method of modal combination was used for the dynamic analysis.

3.5.2 Modelling for Nonlinear Analysis

Modelling walls with plate element performs well in linear analysis but it is difficult to model nonlinear element properties with the plate modelling. Hence the building was modelled with equivalent frame (line) element for the non-linear analysis. The whole building modelled as combination of one dimensional piers and spandrels. The wall portion in between two openings is considered as pier and the portion above and below the opening is considered as spandrel. Width of pier is taken as clear distance between adjacent openings and depth of the pier is taken as thickness of wall. Depth of spandrel is

taken as depth of wall segment available above or below opening and thickness is taken same as wall thickness. Young's modulus of the material is suitably modified in this model to match the elastic modal properties of the building. All other material constants kept similar to that of brick masonry. All the frame elements (piers and spandrels) are modelled with nonlinear properties at the possible yield locations.

In the implementation of nonlinear static (pushover) analysis, the model must account for the nonlinear behaviour of the structural elements. In the present study, a point-plasticity approach is considered for modelling nonlinearity, wherein the plastic hinge is assumed to be concentrated at a specific point in the frame member under consideration. Piers elements in this study were modelled with shear (V2 and V3) hinges at possible plastic regions under lateral load (i.e., both ends of the piers). The normalised force-deformation relations and the acceptance criteria for the hinges were obtained from ASCE/SEI 41-06.

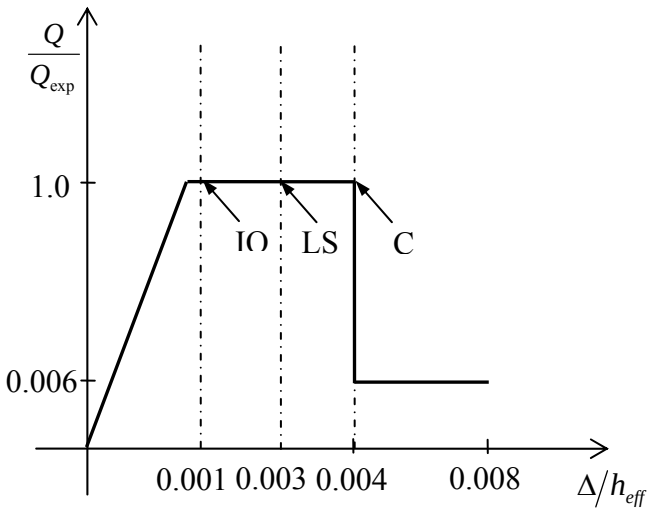

Fig. 3.28 Typical force-deformation relations for plastic hinges (ASCE/SEI 41-06)

The force-deformation relations were taken as symmetric in the positive and negative sides of the shear-force axis. The force-deformation relation and the acceptance criteria for plastic hinge deformation in the piers and spandrels sections are shown in Fig. 3.28.

3.5.3 Comparison of the Pushover Analysis (ASCE/SEI 41-06) with Experimental Analysis Results

Pushover analyses were carried out for all the models as per the procedure outlined in the manuals ASCE/SEI 41-06. Figs. 3.29 and 3.30 present load-deformation responses of two typical walls as obtained from pushover analysis. The experimental results for corresponding walls are also shown for comparison. The responses for other fourteen walls are also found to be identical.

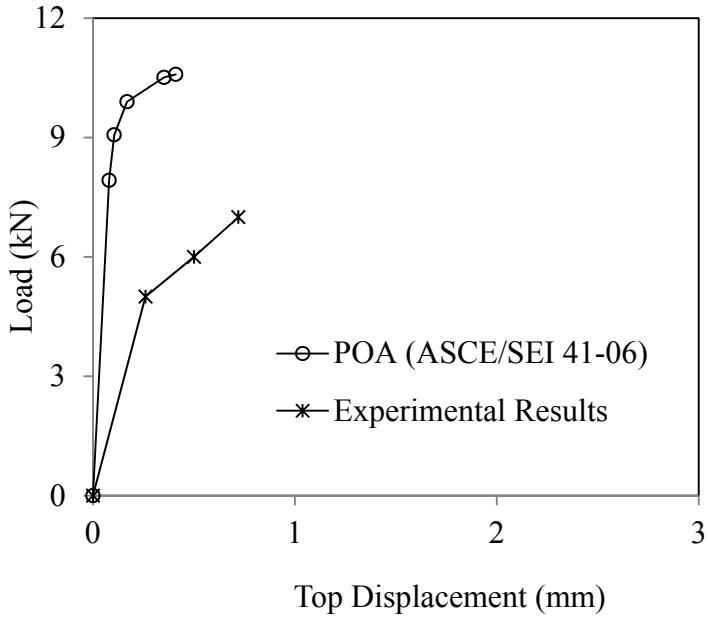

Fig. 3.29 Comparison of experimental and pushover analysis results for Wall Panel W1

These two figures show that the initial stiffness of the wall estimated by the nonlinear static analysis as per ASCE/SEI 41-06 is quite high. This leads to a lesser displacement response by the wall models. Also, the shear strength estimated by the nonlinear static analysis as per ASCE/SEI 41-06 is found to be more than the experimental results.

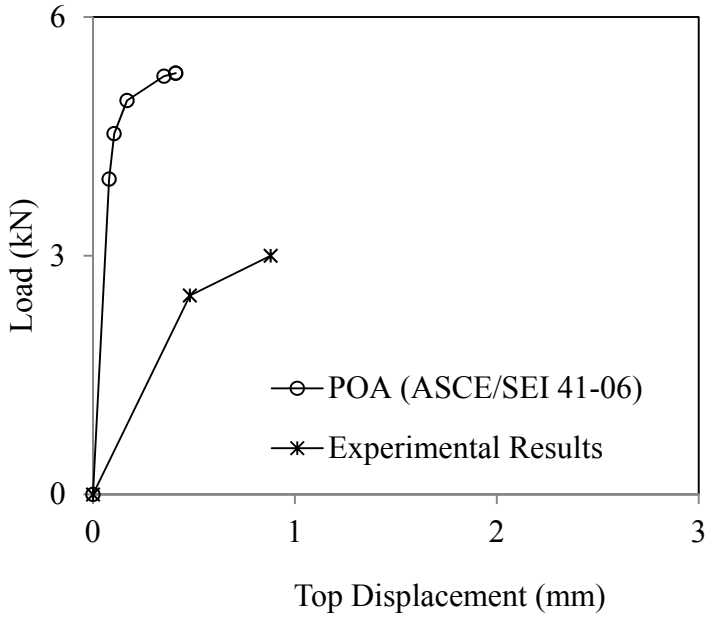

Fig. 3.30 Comparison of experimental and pushover analysis results for Wall Panel W5

3.6 IMPROVED PUSHOVER ANALYSIS FOR URM WALL PANELS

To predict the lateral load-deformation response of URM wall better through pushover analysis some modification over the pushover analysis procedure outlined in ASCE/SEI 41-06 is proposed. There are multiple modifications proposed with regard to structural modelling and hinge modelling of URM wall. The proposed modification is listed as follows:

i) When a two dimensional wall is divided into segments of piers and spandrels and modelled with one-dimensional line elements, the stiffness of the actual wall may get altered. Therefore to model a wall with one dimensional line elements requires suitable material properties that will keep the total elastic stiffness of the wall unaltered. To ensure this Young's modulus of the material is needs to be suitably modified to match the elastic modal properties of the two-dimensional wall segment. All other material constants should be kept similar to that of brick masonry.

ii) The piers and the spandrels should be modelled with cracked section modulus instead of gross section modulus. Cracked moment of inertia of URM wall is found to be 40% of the gross moment of inertia of the same section.

iii) The expected shear strength of URM wall can be divided in to two parts: first part is the strength coming from mortar-brick joint and the second part is due to the presence of axial force on the wall. However, ASCE/SEI 41-06 considers on the second part to calculate expected shear strength of the wall as shown in the following equation:

$$Q_{CE} = 0.9\alpha P_D\left(\frac{L}{h_{eff}}\right) \tag{3.1}$$

Here, Q_{CE} is the expected shear strength of the unreinforced masonry wall. α is a dimensionless coefficient (generally taken as 0.5), P_D is the axial force acting on the wall, L is the length and h_{eff} is the effective height of the wall. In contrary to this the experimental results show that there is a contribution of the mortar brick joint to the shear strength of a URM wall even when there is

no axial force presents. To take this in to account the following relation is established by careful observation of the experimental results.

$$Q_{CE} = 0.9\left[\tau l_{eff} t + \alpha P_D\left(\frac{L}{h_{eff}}\right)\right] \tag{3.2}$$

Here, τ is the shear stress capacity of the unreinforced masonry wall generally taken as 1.75 MPa. l_{eff} is effective length of the wall (total length of the wall minus the length of the opening), t is the thickness of the wall. Also, under lateral load the axial stress in a wall may not be uniform over its cross section. Therefore, it is not proper to depend on the axial force too much for assessing the shear strength of a wall segment in a URM wall building. A value of $\alpha = 0.2$ is arrived using trial and error method to fit the experimental results presented here.

Pushover analyses carried out on all the wall models considering the above modifications. The resulting pushover curves were plotted with the experimental results and presented in Figs. 3.31 – 3.42

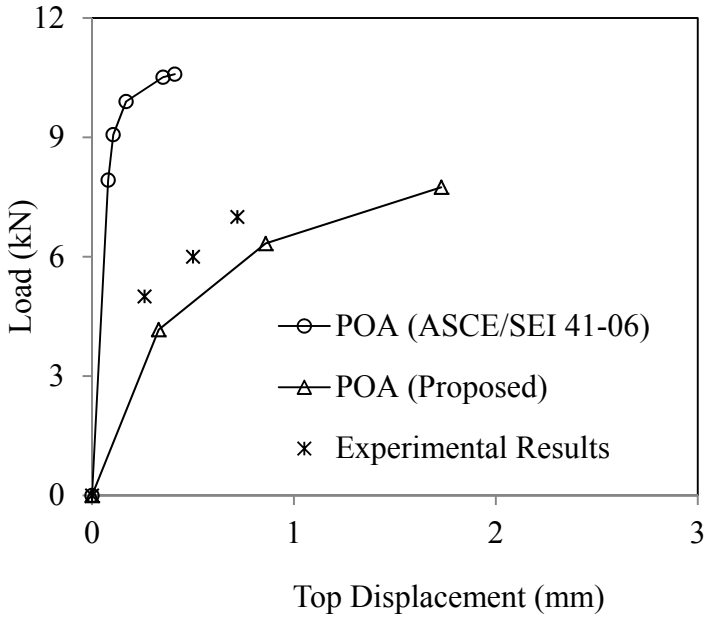

Fig. 3.31 Comparison of capacity curves for Wall Panel W1

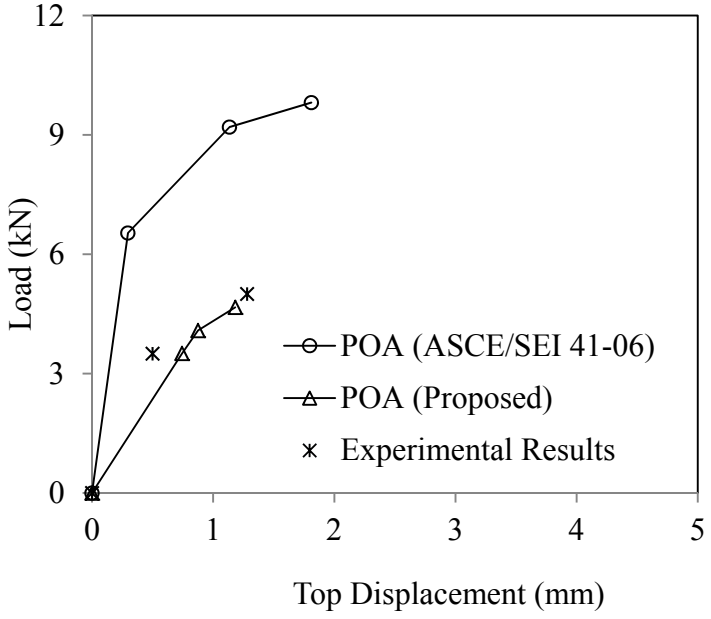

Fig. 3.32 Comparison of capacity curves for Wall Panel W2

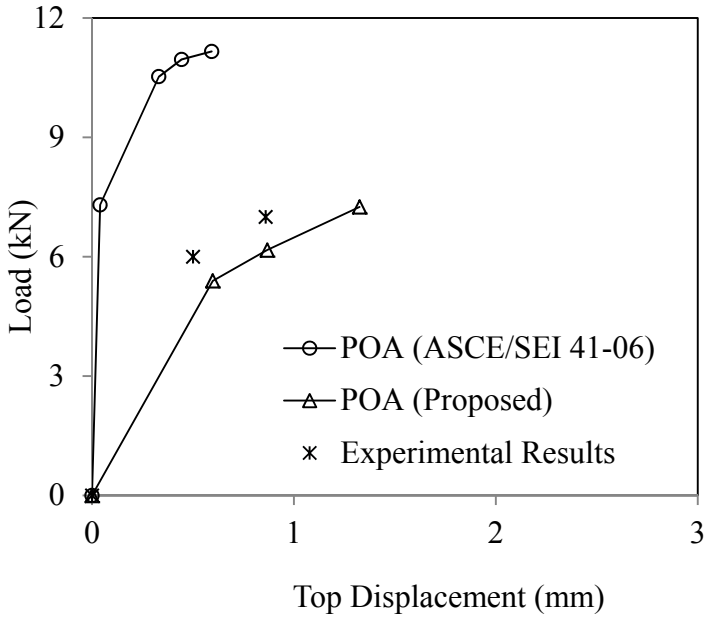

Fig. 3.33 Comparison of capacity curves for Wall Panel W3

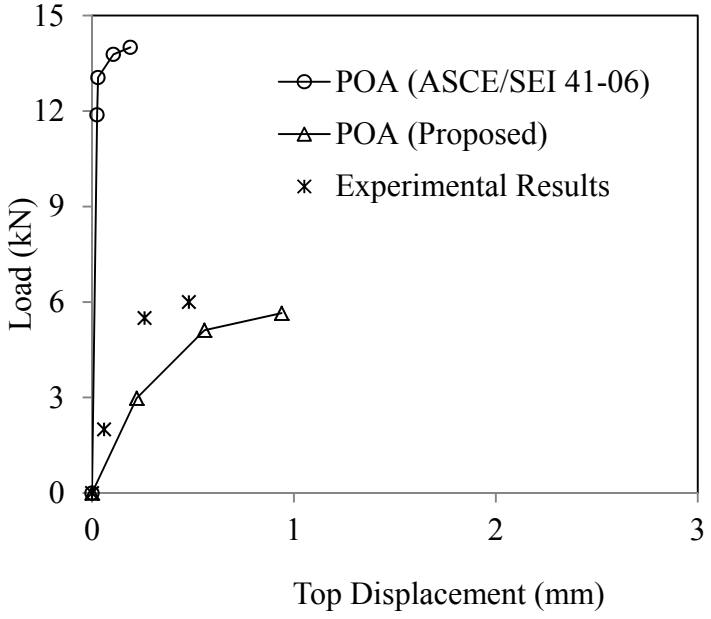

Fig. 3.34 Comparison of capacity curves for Wall Panel W4

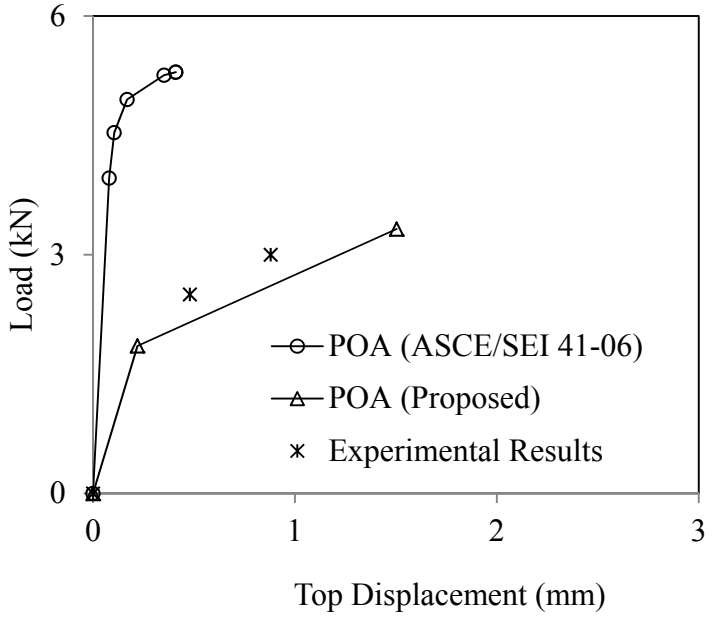

Fig. 3.35 Comparison of capacity curves for Wall Panel W5

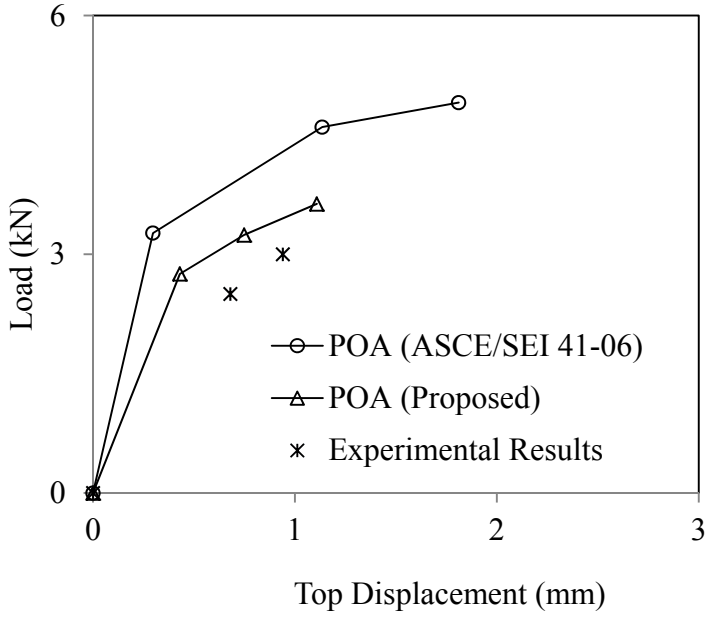

Fig. 3.36 Comparison of capacity curves for Wall Panel W6

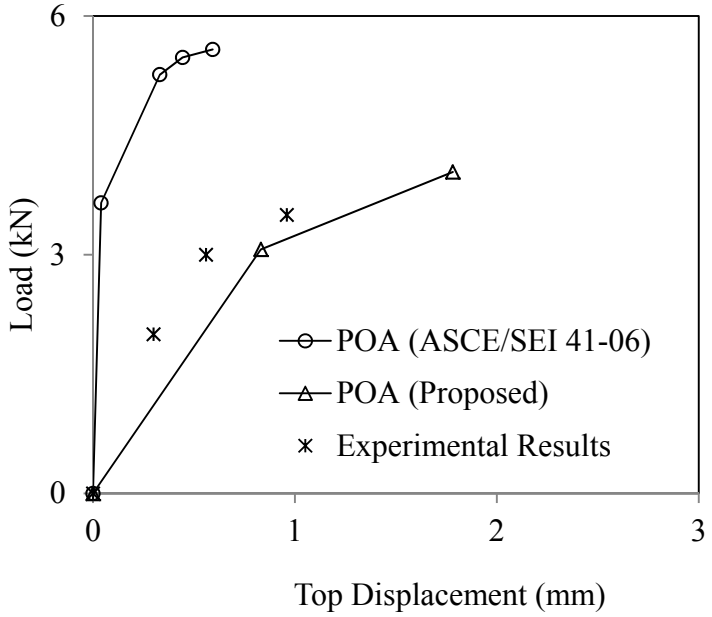

Fig. 3.37 Comparison of capacity curves for Wall Panel W7

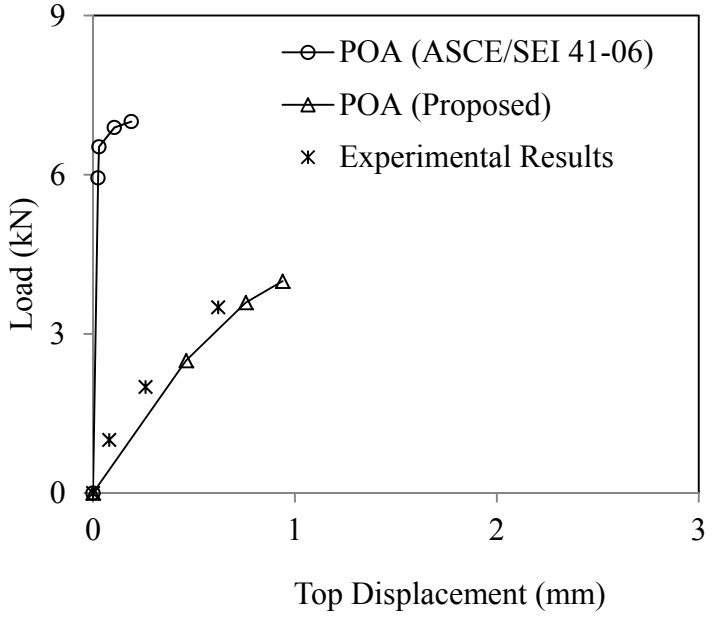

Fig. 3.38 Comparison of capacity curves for Wall Panel W8

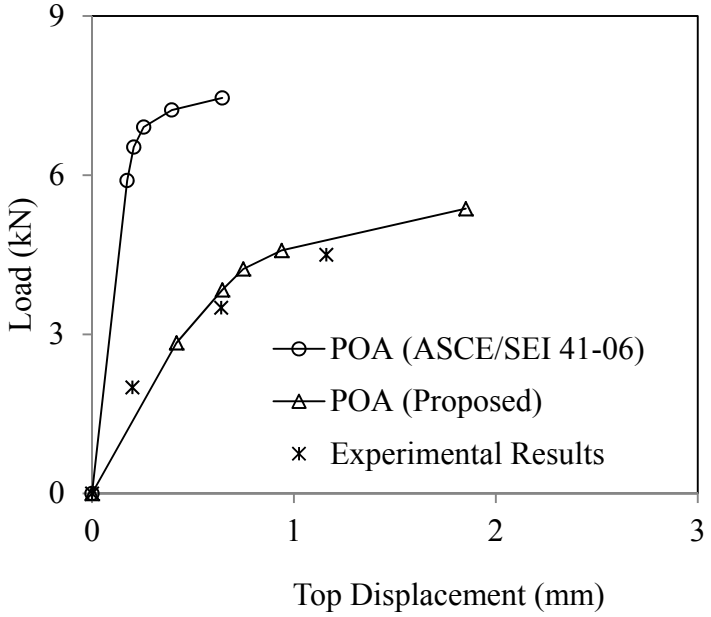

Fig. 3.39 Comparison of capacity curves for Wall Panel W9

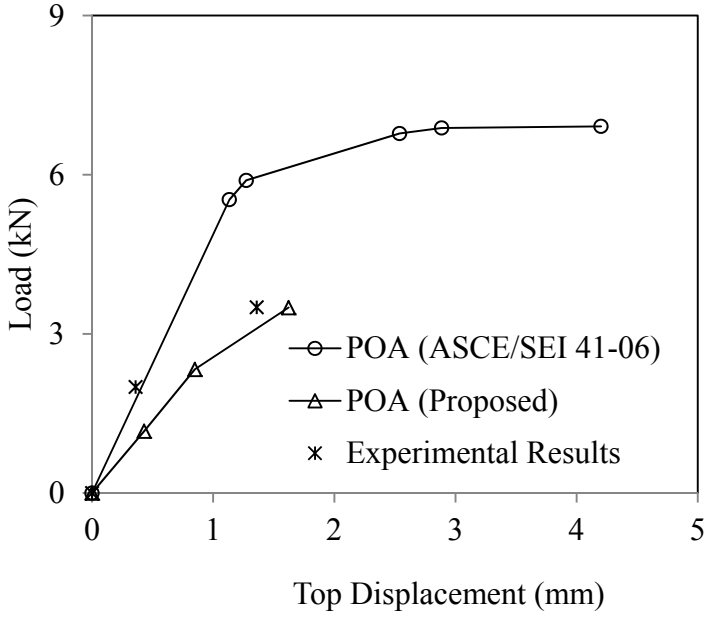

Fig. 3.40 Comparison of capacity curves for Wall Panel W10

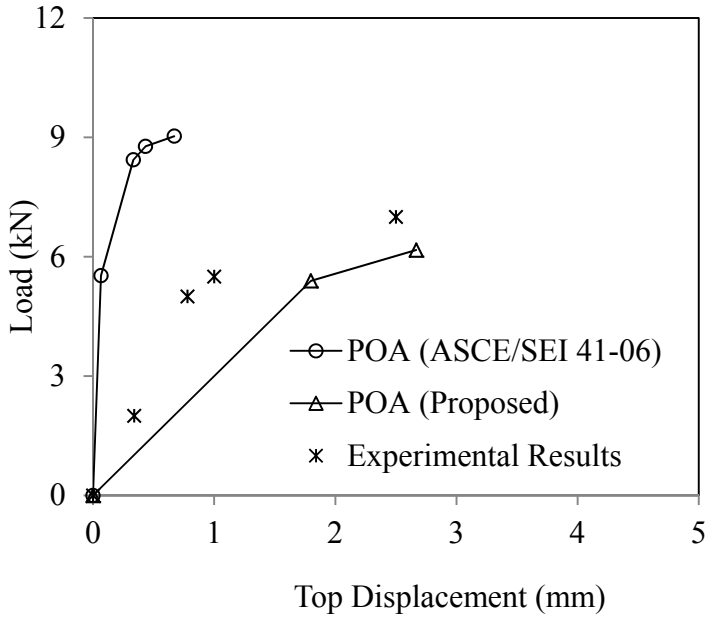

Fig. 3.41 Comparison of capacity curves for Wall Panel W11

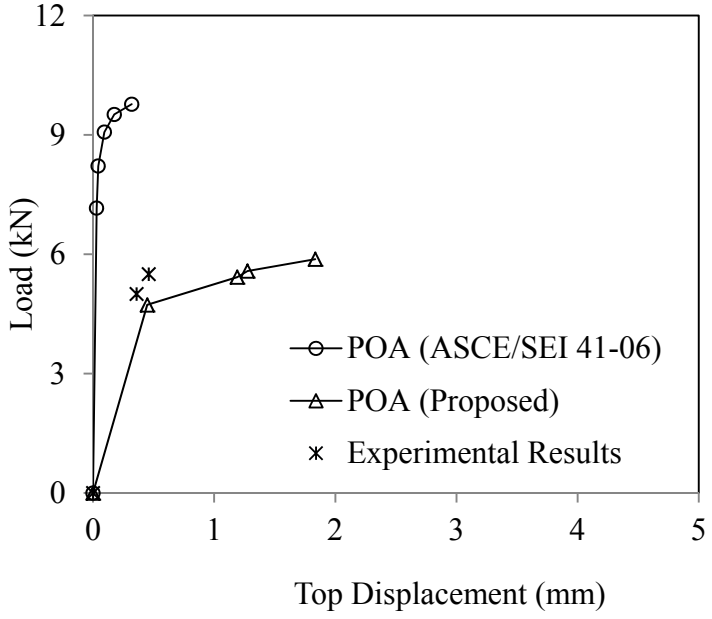

Fig. 3.42 Comparison of capacity curves for Wall Panel W12

The figures presented here show that the results of pushover analysis with proposed modifications closely match the experimental results. It is to be noted that the proposed method slightly underestimates the base shear capacity (with a variation up to 10%), which is conservative.

3.6.1 Pushover Curve Error Index

"Pushover curve error index" (E_{PC}) is introduced as a measure of the discrepancy between the pushover analyses and experimental results in terms of base shear versus roof displacement relation. It is numerically simple and very efficient to define the difference between the ordinates of a pushover curve and the base shear versus roof displacement response obtained from the experimental results for the same wall panels. This is based on a similar concept due to standard error of displacement profile (Menjiver, 2004).

Consider the pushover curve $S_0 - S_4$ and the set of points obtained from experimental analysis $D_1 - D_5$ in Fig. 3.43. The coordinates of the vertical projection of each experimental result point on the pushover curve are calculated by linear interpolation between neighbouring pushover points. Points with no projections (like D_5 in Fig. 3.43) are ignored. The pushover curve error index (E_{PC}) is calculated using the following equation:

$$E_{PC} = \sqrt{\frac{1}{N}\sum_{1}^{N}\left(\frac{d_i}{Y_{Di}}\right)^2} \qquad (4.14)$$

where d_i is the vertical projection of the i^{th} experimental result point on the pushover curve, Y_{Di} is the Y-coordinate of i^{th} experimental result point and N is the total number of points considered.

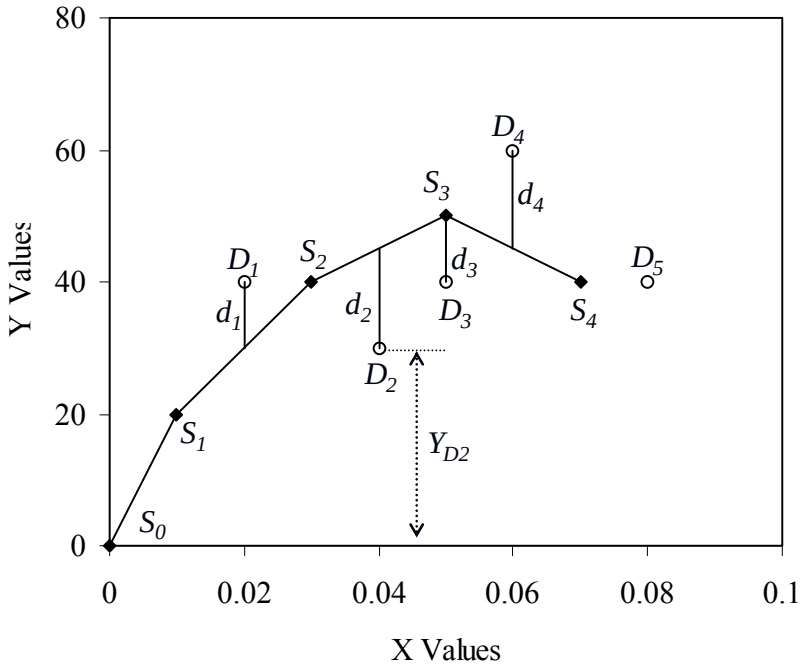

Fig. 3.43: Definition of pushover curve error index

A value of pushover curve error index approaching to zero implies high accuracy in the pushover analysis results (proximity to the experimental results). Table 3.4 presents the pushover curve error index for different frames for various load patterns used in pushover analysis. The table shows that proposed profile predicts results with more accuracy compared to the ASCE/SEI 41-06.

3.7 SUMMARY

This chapter begins with the description of the experimental program carried out as part of this research. It includes the experimental setup, details of the test specimens and the results obtained from the experimental investigations.

Table 3.4: Pushover curve error index

Wall ID	ASCE/SEI 41-06	Proposed
W1	0.86	0.14
W2	0.84	0.07
W3	0.86	0.10
W4	5.53	0.34
W5	1.11	0.12
W6	0.53	0.30
W7	1.29	0.12
W8	2.50	0.03
W9	1.13	0.07
W10	0.68	0.30
W11	2.34	0.12
W12	0.95	0.14
Mean Error	1.55	0.15

This chapter then presents an evaluation of existing pushover analysis method (ASCE/SEI 41-06) for URM building. The results show that this method overestimates the strength and stiffness of the URM wall. A set of modification is proposed for the pushover analysis of URM building based on the experimental investigation. These proposed modifications show consistently good performance in comparison with the existing method (ASCE/SEI 41-06) of pushover analysis.

CHAPTER 4

SEISMIC EVALUATION CASE STUDY OF AN EXISTING UN-REINFORCED MASONRY BUILDING

4.1 INTRODUCTION

In this chapter, an existing URM building from Guwahati, India (Zone V) is presented as a case study. The building was analysed using equivalent static method; response spectrum method (IS 1893: 2002) followed by pushover analysis as per ASCE/SEI 41-06 with proposed modification. It was found that, based on the linear analysis the building does not satisfy the requirements of the current IS code (IS 1905:1987). Of course the nonlinear pushover analysis results reveal that the building has sufficient strength and ductility at global levels.

4.2 BUILDING DESCRIPTION

An existing load bearing unreinforced masonry building located in Guwahati (seismic zone V) presented in this paper. Figs. 4.1 and 4.2 show the typical floor plan and 3D computer model of the building respectively. It is a two storey residential buildings (2×3.2m height from the ground level) with door and window openings. Plan dimensions of the building are 11.4m × 9.5m. Standard brick of size 230mm × 110mm × 75mm and mortar grade of M1 (IS 1905:1987) were used for the construction of the building using Flemish Garden wall bond (IS 2212:1991). The building is approximately five years old. Thickness of all the outer walls is 230mm and all inner walls are of 110mm thick. The slabs are 150mm thick for all the floor levels in the buildings. Visual inspection did not reveal any deterioration in buildings. The sub-soils were assumed to be medium (Type II) as geotechnical data were not available. Walls were supported on 350 thick

and 1000mm deep brick wall.

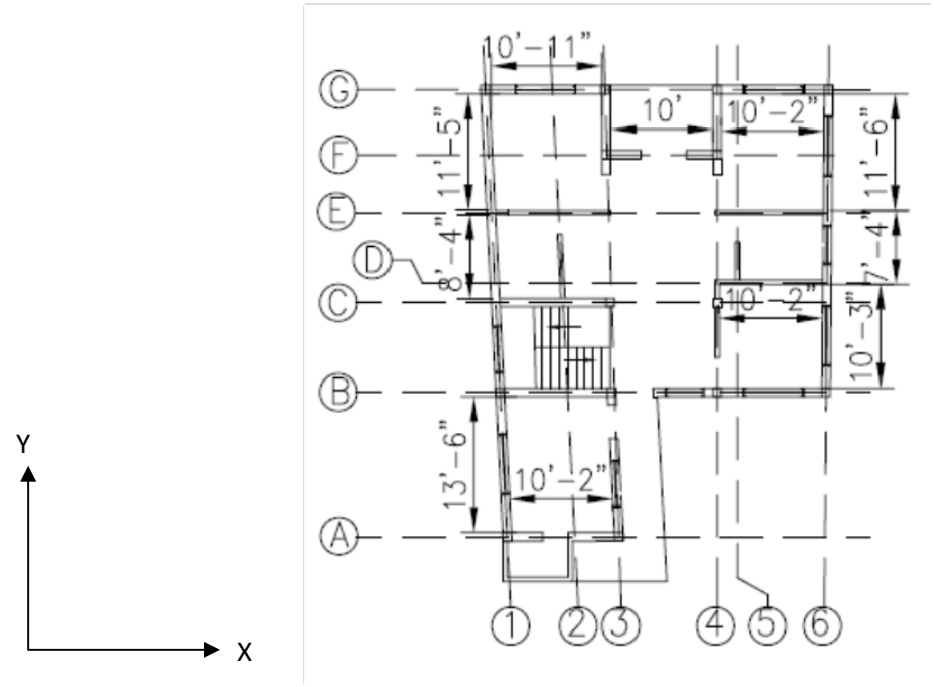

Fig. 4.1**:** Typical floor plan with the gridlines of the Building

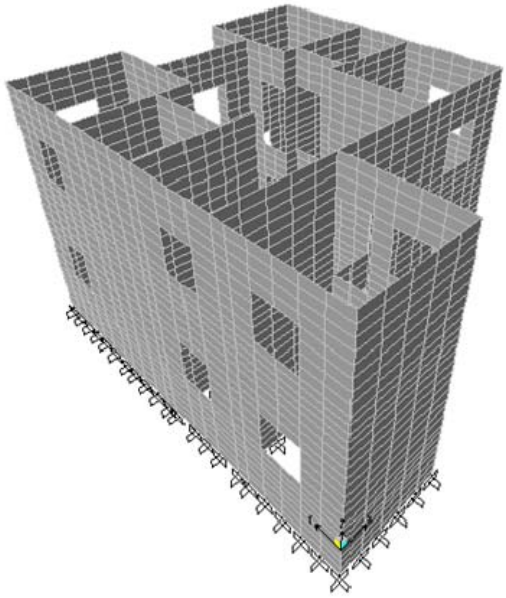

Fig. 4.2**:** 3D computer model of the Building

4.3 RESULTS AND DISCUSSIONS

The building model was analysed using Equivalent Static Method (linear static method) and Response Spectrum Method (linear dynamic method) according to IS 1893:2002. Pushover Analysis (nonlinear static method) was also carried out. The pushover analysis provides an insight into the structural aspects which control the performance during earthquakes. It also provides data on the strength and ductility of a building. The analyses were done by using the finite element analysis software, SAP2000. All the three analyses expose various design weaknesses that are present in a building.

To evaluate the performance of this building, a performance based approach was adopted. The performance based approach identifies a target building performance level under an anticipated earthquake level. The building performance is broadly categorized under the levels of (a) collapse prevention, CP, (b) life safety, LS, and (c) immediate occupancy, IO. The two commonly used earthquake levels are design basis earthquake (DBE) and maximum considered earthquake (MCE). For the present buildings, CP under MCE was selected as the safety objective.

Table 4.1: Time periods and modal participation for the first three modes

Mode	Natural Period (s)	Mass Participation Ratio (%)	
		UX	UY
1	0.075	43	19
2	0.069	22	46
3	0.054	02	04

Table 4.1 provides the period and the predominant direction of vibration for the first three modes of the building as obtained from the modal analysis of the elastic model. The table also shows the

percentage of mass participation for each of the three modes. It is clear from the table that all the three modes are coupled translational-torsional mode. This is due to the irregular shape of the building in plan and irregular opening distribution in the wall. As the base shear found in response spectrum analysis (V_B) is lesser than design base shear ($\overline{V}_B$) as per IS 1893:2002, shear stress demand from response spectrum analysis was scaled up by a factor equal to the ratio of the two base shears ($\overline{V}_B/V_B$). Table 4.2 shows the comparison between (V_B) and ($\overline{V}_B$).

Table 4.2: Comparison of Base Shear

	$V_x(kN)$	$V_y(kN)$
Equivalent Static $\left(\overline{V_B}\right)$	575.8	575.8
Response Spectra $\left(V_B\right)$	236.94	237.52
$\overline{V_B}/V_B$	2.43	2.42

The absolute shear demand for each wall segment was calculated from elastic analyses for the load combinations given in IS-1893: 2002 and compared with the corresponding capacities in terms of Demand Capacity Ratio (DCR). DCR refers the ratio of the shear stress demand to the shear stress capacity for a wall segment. Shear capacity for the brick masonry walls were calculated (IS 1905:1987) as follows:

$$f_s = 0.1 + \frac{f_d}{6} \tag{1}$$

Where f_s is shear strength (in MPa) and f_d is the compressive stress acting on the wall (in MPa) due to dead load. For each wall segment maximum demand was calculated by equivalent static, response spectrum methods and thereby DCR calculated for all wall segments. For typical walls, shear stress demand and capacities were tablulated in Table 4.3. This table show that a number of

wall segment do not satisfy the code criteria as the corresponding DCR values exeed 0.9. To include the detoriaration of the structural material a lesser DCR (less than 1.0) is taken as the criterion for code compliance. But for the present building, maximum wall segments exeeds the permissible limit of DCR value.

Table 4.3: Deficient walls in the building

Wall Grid		Shear strength (MPa)	Equivalent Static Analysis		Response spectrum analysis	
			Shear Demand (MPa)	DCR	Shear Demand (MPa)	DCR
X- Panels						
Ground Floor Walls	B3-B4	0.12	0.30	2.5	0.29	2.0
	D4-D6	0.14	0.21	1.5	0.23	1.6
	E1-E3	0.14	0.23	1.6	0.25	1.9
	F3-F4	0.12	0.35	3.0	0.37	3.2
1st Floor Walls	B3-B4	0.12	0.26	2.4	0.24	2.1
	D4-D6	0.14	0.14	1.2	0.12	1.1
	E1-E3	0.14	0.14	1.2	0.11	1.0
	F3-F4	0.12	0.30	2.9	0.26	2.5
Y- Panels						
Ground Floor Walls	A3-B3	0.15	0.21	1.4	0.25	1.7
	B4-C4	0.13	0.19	1.4	0.20	1.5
	B6-D6	0.14	0.41	2.9	0.49	3.5
	G1-E1	0.12	0.29	2.3	0.26	2.2
1st Floor Walls	A3-B3	0.15	0.21	1.7	0.16	1.3
	B4-C4	0.13	0.13	1.2	0.09	0.8
	B6-D6	0.14	0.34	2.8	0.31	2.6
	G1-E1	0.12	0.19	1.7	0.17	1.6

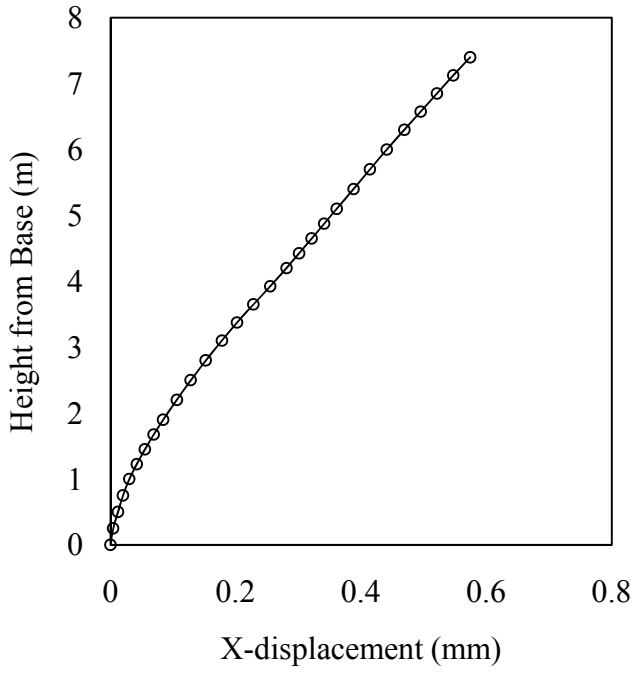

Fig. 4.3: Displacement profile of the building under design lateral force along X-axis

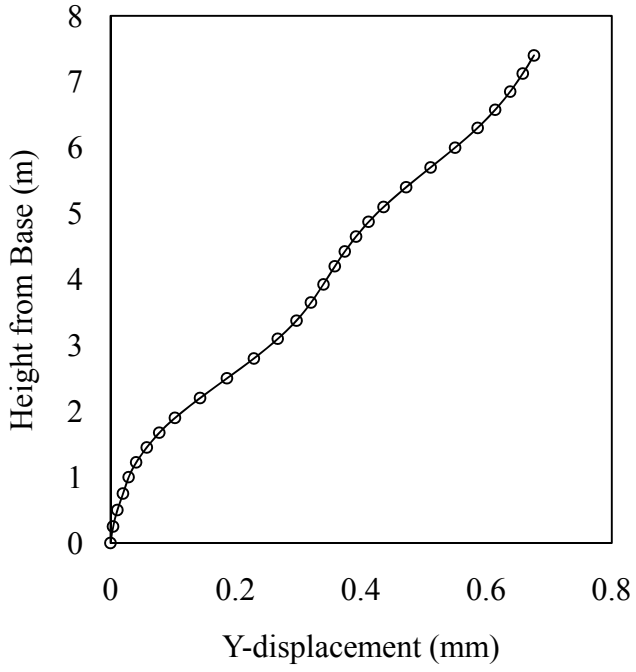

Fig. 4.4: Displacement profile of the building under design lateral force along Y-axis

Displacement profile of the building under design lateral force along X- and Y- axes are shown in Figs. 4.2-4.3. The storey drift for every storey due to the design lateral force, with partial load factor of 1.0, calculated. For both the direction inter-storey drift is within the code limitation of 4%. Fig. 4.4 shows storey drift in both the directions when design seismic force applied in the respective direction.

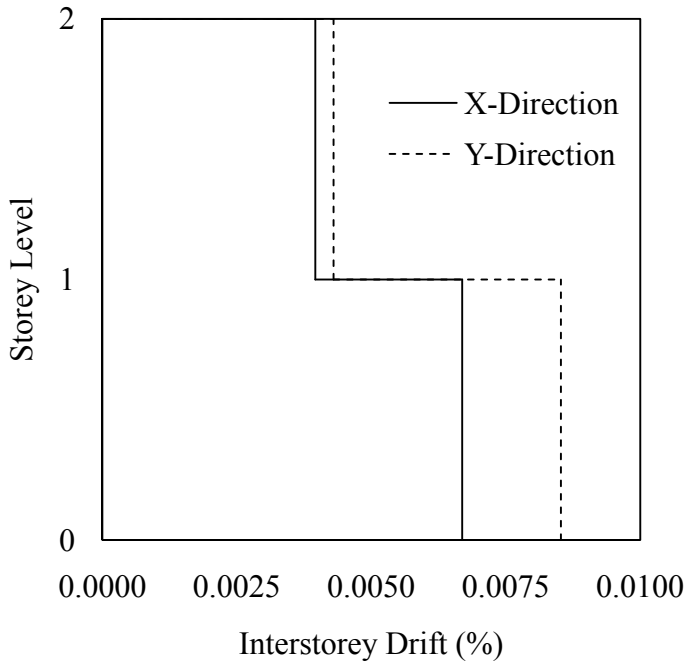

Fig. 4.5: Storeydrifts for design seismic base shear

Pushover analysis is done for the gravity loads (DL+0.25LL) incrementally under load control. The lateral pushover analysis (in X- and Y- directions) was followed after the gravity pushover, under displacement control. The building is pushed in lateral directions until the formation of collapse mechanism. The pushover curve (Base shear versus Roof displacement) is obtained in X- and Y- directions and presented in Fig. 4.5.

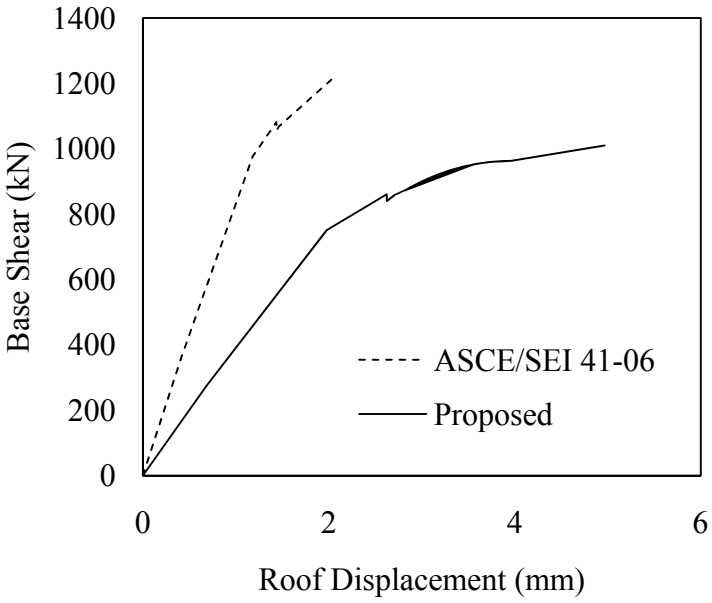

(a) X- direction push

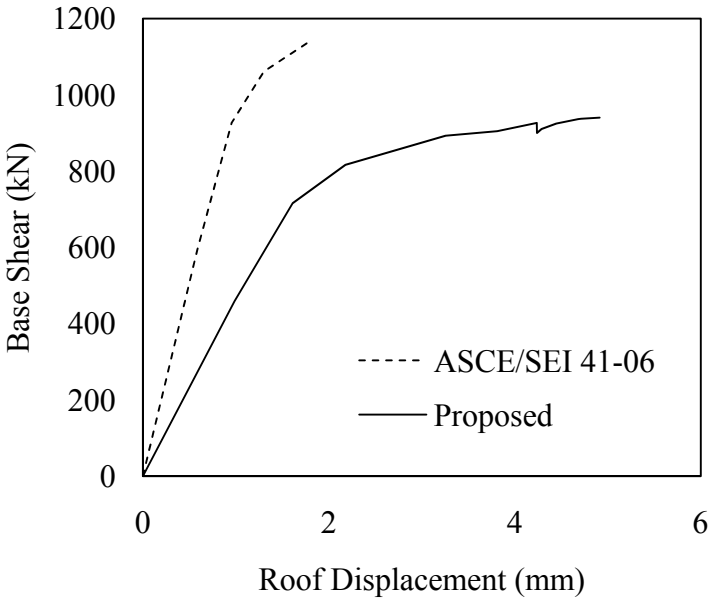

(b) Y- direction push

Fig. 4.6: Pushover curve of the building

Pushover curve shows that, as per ASCE/SEI 41-06, the base shear capacities of the building along X- and Y- directions are 1,217 kN (*i.e.*, 60% of total weight) and 1,142 kN (*i.e.*, 58% of total weight) respectively. However results of the pushover analysis with proposed modifications found to be conservative with respect to the conventional pushover analysis. The proposed method predicts lesser base shear capacity with lesser elastic stiffness of the URM building.

This figure shows that the building strength comfortably reaching the design base shear force ($\overline{V}_B = 575.8\ kN$) in both the directions as per both the methods. Maximum roof displacements, as per ASCE/SEI 41-06, along X- and Y- directions are 2.05mm (0.028% of the building height) and 1.81mm (0.024% of the building height) respectively. These values for the proposed method are 4.96mm (0.067% of the building height) and 4.93mm (0.067% of the building height) along X- and Y- directions respectively

Target displacements for the building were calculated as per ASCE/SEI 41-06 and presented in Table 4.4. Formation of the hinges during pushover analysis shows that the failure of the building is due to the failure of the ground storey walls and subsequent formation of storey mechanism.

Table 4.4: Target displacement (mm) for the building (ASCE/SEI 41-06)

	Life Safety (LS)	Collapse Prevention (CP)	Displacement undergone
X-direction	2.44	2.87	4.21
Y-direction	2.02	2.38	3.10

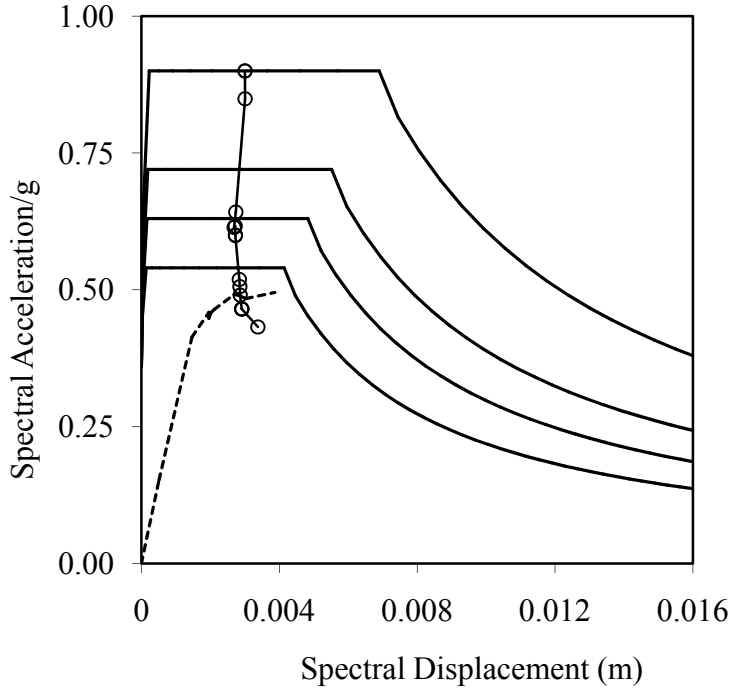

(a) X- direction push

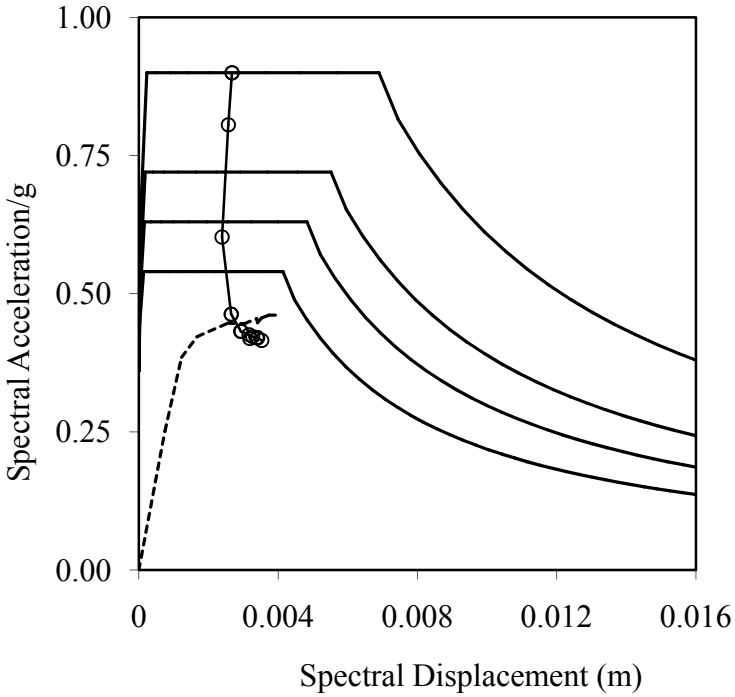

(b) Y- direction push

Fig. 4.7: Capacity and demand spectrum under MCE

In a pushover analysis, when the demand spectrum is plotted along with the capacity spectrum in an Acceleration Displacement Response Spectrum (ADRS) format, the two curves may meet to give a performance point. Capacity spectrum here corresponds to the base shear versus roof displacement curve. This approach is to check the performance of the building as per capacity spectrum method given in ATC-40. The zone factor (Z) for Guwahati is taken as 0.36. The demand spectrum for MCE is obtained from peak ground acceleration (PGA) of 0.36g. The demand spectrum is plotted with C_a = 0.36g, C_v= 1.36×0.36g, and 5% initial damping. The demand spectrum is compared with the capacity spectrum and is shown in Fig. 4.6.

Table 4.5: Status of performance point for MCE

Quantity	Value	Quantity	value
Pushover along X-axis			
Base Shear (kN)	960 (50%W)	Roof displacement (mm)	3.77 (0.05%H)
Spectral acceleration, S_a (m/s^2)	0.489	Spectral displacement, S_d (mm)	2.866
Effective time period, T_{eff} (s)	0.154	Effective damping, β_{eff}	0.207 (20.7%)
Pushover along Y-axis			
Base Shear (kN)	898 (47%W)	Roof displacement (mm)	3.53 (0.05%H)
Spectral acceleration, S_a (m/s^2)	0.446	Spectral displacement, S_d (mm)	2.79
Effective time period, T_{eff} (s)	0.159	Effective damping, β_{eff}	0.239 (23.9%)

The performance point is achieved in this case which is the point at which demand and capacity meets. The base shear, roof displacement, spectral acceleration, spectral displacement, effective time period and effective damping corresponding to the performance point are given in Table 4.5. For the present building, pushover analysis in both directions gave a performance point. So the global performance of the building is acceptable as per ATC-40 capacity spectrum

method. So the building does not need retrofitting in a global sense but some of the wall segments need local retrofitting as plastic hinges on those sections are going beyond life-safety limit. The formation of hinges at performance point in a typical frame is shown in the Fig. 4.7.

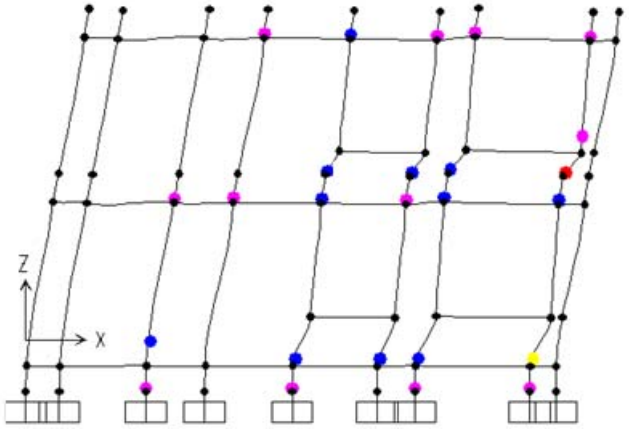

(a) X- direction push

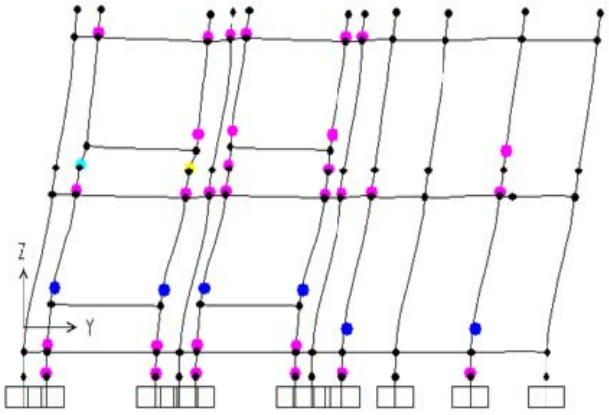

(b) Y- direction push

Fig. 4.8: Formation of hinges at performance point

4.4 CONCLUSIONS

This chapter illustrates the methodology for the seismic evaluation of unreinforced masonry buildings through a case study. A two-story existing unreinforced masonry building from Guwahati is selected for the case study. The use of pushover analysis as a tool of evaluating the seismic performance is illustrated. The pushover analyses of the selected building is carried out as per ASCE/SEI 41-06 with proposed modification. The main conclusion from the study is that proposed modifications of pushover analysis on ASCE/SEI 41-06 method result in conservative estimations.This also illustrates that thethe performance based evaluation is a rational tool for seismic evaluation of unreinforced masonry buildings. Pushover analysis is an elegant method for visualizing the damage state of a building.

CHAPTER 5

SUMMARY AND CONCLUSIONS

5.1 SUMMARY

Inadequacies of many un-reinforced masonry (URM) buildings have been realized in recent earthquakes in India and hence method of ensuring adequacy of such buildings is of urgent need. Although a considerable research is directed to study the reinforced concrete building, there is no structured methodology to assess the URM building in our country is available. It is important to develop systematic method of evaluation of existing URM buildings. With this background the main objectives of this research were defined as: i) to assess pushover analysis methodology prescribed in ASCE/SEI 41-06 for unreinforced masonry buildings through experimental investigation and to propose improvement if required, ii) to develop equivalent frame model for nonlinear analysis of URM building, and iii) to carry out a case study of seismic evaluation of an existing URM building using the improved pushover analysis.

To achieve the above objectives, a detailed literature review on unreinforced masonry buildings was first carried out. This also includes the design code perspectives on unreinforced masonry buildings. The literature review is presented in Chapter 2.

An experimental program has been carried out as part of this research. The experimental setup, details of the test specimens and the results obtained from the experimental investigations are discussed in Chapter 3.

An evaluation of existing pushover analysis method (ASCE/SEI 41-06) for URM building is also carried out. The results show that this method overestimates the strength and stiffness of the URM wall. A set of modification is proposed for the pushover analysis of URM building based on the experimental investigation. These proposed modifications show consistently good performance in comparison with the existing method (ASCE/SEI 41-06) of pushover analysis.

Finally an existing URM building from Guwahati, India (Zone V) is presented as a seismic evaluation case study. The building was analysed using equivalent static method; response spectrum method (IS 1893: 2002) followed by pushover analysis as per ASCE/SEI 41-06 with proposed modification. It was found that, based on the linear analysis the building does not satisfy the requirements of the current IS code (IS 1905:1987). Of course the nonlinear pushover analysis results reveal that the building has sufficient strength and ductility at global levels.

5.2 CONCLUSIONS

Based on the work presented in this thesis following point-wise conclusions can be drawn:

i) Modelling walls with plate element performs well in linear analysis but it is difficult to model nonlinear element properties with the plate modelling. Hence the URM building has to be modelled with equivalent frame (line) element for the non-linear analysis. The wall portion in between two openings should be considered as pier and the portion above and below the opening should be considered as spandrel. Width of pier is the clear distance between

adjacent openings and depth of the pier is the thickness of wall. Similarly depth of spandrel should be the depth of wall segment available above or below opening and thickness is same as wall thickness.

ii) The total stiffness of the URM building is going to be altered (reduced) due to the frame modelling as the connectivity gets reduced in the frame model. To account for this reduction in stiffness Young's modulus of the material needs to be suitably modified in frame model to match the elastic modal properties of the URM building building. All other material constants can be kept similar to that of brick masonry.

iii) The piers and the spandrels should be modelled with cracked section modulus instead of gross section modulus. Cracked moment of inertia of URM wall is found to be 40% of the gross moment of inertia of the same section.

iv) Experimental results show that the pushover analysis procedure given in ASCE/SEI 41-06 for URM wall panels is un-conservative for strength and stiffness estimation.

v) The expected shear strength of URM wall can be divided in to two parts: first part is the strength coming from mortar-brick joint and the second part is due to the presence of axial force on the wall. However, ASCE/SEI 41-06 considers on the second part to calculate expected shear strength of the wall as shown in the following equation:

$$Q_{CE} = 0.9\alpha P_D \left(\frac{L}{h_{eff}} \right)$$

Here, Q_{CE} is the expected shear strength of the unreinforced masonry wall. α is a dimensionless coefficient (generally taken as 0.5), P_D is the axial force acting on the wall, L is the length and h_{eff} is the effective height of the wall. In contrary to this the experimental results show that there is a contribution of the mortar brick joint to the shear strength of a URM wall even when there is no axial force presents. To take this in to account the following relation is established by careful observation of the experimental results.

$$Q_{CE} = 0.9\left[\tau l_{eff} t + \alpha P_D \left(\frac{L}{h_{eff}}\right)\right]$$

Here, τ is the shear stress capacity of the unreinforced masonry wall generally taken as 1.75 MPa. l_{eff} is effective length of the wall (total length of the wall minus the length of the opening), t is the thickness of the wall. Also, under lateral load the axial stress in a wall may not be uniform over its cross section. Therefore, it is not proper to depend on the axial force too much for assessing the shear strength of a wall segment in a URM wall building. A value of $\alpha = 0.2$ is arrived using trial and error method to fit the experimental results presented here.

5.3 SCOPE OF FUTURE STUDY

i) The present study is limited to masonry walls made of burnt clay bricks with sand-cement mortar. However, there is an increasing trend of using fly ash bricks in the URM brick masonry. This study can be extended to masonry walls made of fly ash bricks.

ii) Estimation of target displacement in pushover analysis of URM building is another area that needs attention. ASCE/SEI 41-06 is not very clear about this.

iii) There is no specific recommendation in ASCE/SEI 41-06 for the use of lateral load pattern for carrying our pushover analysis of URM building. There is a scope for future work in this area.

iv) There is a scope of research on the behaviour of vertical and plan irregular URM building.

REFERENCES

1. **Abrams, D. P. (1992), "***Strength and Behaviour of Un-reinforced Masonry Elements***",** 10th world conference on Earthquake Engineering, Balkema, Rotterdam.

2. **Agarwal, P. and Takkar, S. K. (2001),** "A comparative Study of Brick Masonry House Model Under Quasi-Static and Dynamic Loading", *Journal of Earthquake technology*, vol. 38, pp. 103-122.

3. **Arioglu, E. and Anadol, K. (1973),** *"The Structural Performance of Rural Dwellings during Recent Destructive Earthquakes in Turkey (1969 -72)",* 5th world conference on earthquake engineering, Rome.

4. **ASCE/SEI-41 (2006)**, Seismic Rehabilitation of Existing Buildings. American Society of Civil Engineers.

5. **ATC 40 (1996)**, Seismic Evaluation and Retrofit of Concrete Buildings: Vol. 1, Applied Technology Council, USA

6. **Bruneau, M.** (1994) "Seismic evaluation of unreinforced masonry buildings — a state-of-the-art report", *Canadian Journal of Civil Engineering*, vol. 21, no. 3, pp. 512-539

7. **Eurocode 8** (2004), Design of Structures for Earthquake Resistance, Part-1: General Rules, Seismic Actions and Rules for Buildings, European Committee for Standardization (CEN), Brussels.

8. **FEMA 356** (2000), Prestandard and Commentary for the Seismic Rehabilitation of Buildings, American Society of Civil Engineers, USA.

9. **FEMA 440** (2005), Improvement of nonlinearstatic seismic analysis procedures, Applied Technology Council (ATC) Washington, D.C.

10. **FEMA 273** (1997), NEHRP Guidelines for the seismic rehabilitation of buildings. *Federal Emergency Management Agency*, Applied Technology Council, Washington D.C., USA.

11. **FEMA 274** (1997), NEHRP Commentary on the Guidelines for the Seismic Rehabilitation of Buildings. *Federal Emergency Management Agency*, Applied Technology Council, Washington D.C., USA.

12. **Gupta, B.** and **Kunnath, S.K.** (2000). Adaptive spectra-based pushover procedure for seismic evaluation of structures. *Earthquake Spectra*, **16**(2), 367-391.

13. **IS 1893.** (2002). Indian Standard Criteria for Earthquake Resistant Design of Structures, Bureau of Indian Standards, New Delhi.

14. **IS 1905.** (1987) Code of Practice for Structural use of Un-reinforced Masonry, Bureau of Indian Standards, New Delhi.

15. **IS 2212.** (1991). Brick Work - Code of Practice, Bureau of Indian Standards, New Delhi.

16. **IS 3828 (1976),** "*Improving Earthquake Resistance of Low Strength Masonry Buildings – Guidelines"*, Bureau of Indian Standards, New Delhi.

17. **IS 456** (**2000)**. Indian Standard for Plain and Reinforced Concrete - Code of Practice, Bureau of Indian Standards, New Delhi.

18. **Jai Krishna and Brijesh Chandra** (1965), "*Strengthening of Brick Buildings Against Earthquake Forces*", Proceedings 3rd world conference on earthquake engineering, New Zealand, Vol. III, pp. 324-341.

19. **Jurina, L. and Peano, A. (1982).** "Characterization of brick masonry stiffness by numerical modelling and in situ flat-jack test results" Sixth international brick masonry conference. Rome, 16th - 19th may, 1982, Pages 177-188.

20. **Kappos, A. J.; Penelis, G. G. and Drakopoulos C. G. (2002)**, *"Evaluation of Simplified Models for Lateral Load Analysis of Unreinforced Masonry Buildings"*, Journal of Structural Engineering, July, pp. 890-897.

21. **Mebarki, A.; Bui, Q. H.; Sadda, R. A.; Delmotte**, P. and **Tizapa, S. S.** (2008). A simplified mechanical model to assess the bearing capacity of masonry walls: Theory and experimental validation, *Construction and Building Material*, vol. 23, pp. 1109–1117

22. **Menjivar, M.A.L.** (2004). A Review of Existing Pushover Methods for 2-D Reinforced Concrete Buildings. Ph.D. Thesis, ROSE School, Italy.

23. **Mwafy, A.M.** and **Elnashai, S.A.** (2000). Static pushover versus dynamic-to-collapse analysis of RC buildings. Engineering Seismology and Earthquake Engineering Section, Imperial College of Science, Technology and Medicine. Report No. 00/1.

24. **Navalli, S. S.** (2001), "Uttarkashi: Houses that hold on", Down to Earth, Centre for Science and Environment pub.

25. **Paulay, T.** and **Priestley, M. J. N.** (1992). Seismic design of reinforced concrete and masonry buildings, John Wiley and Sons, New York

26. **PCM 3274** (2003). Primi Elementi in Materia di Criteri Generali per la Classificazione Sismica del Territorio Nazionale e di Normative Tecniche per le Costruzioni in Zona Sismica (in Italian), Roma, Italy.

27. **Raghunath, S. (2003)**, *"Static and Dynamic Behaviour of Brick Masonry with Containment Reinforcement"*, PhD thesis, Department of civil engineering, Indian Institute of Science, Bangalore.

28. **Rai, D. C. and Goel, S. C., (1996),** *"Seismic Strengthening of Un-reinforced Masonry Piers With Steel Elements"*, Earthquake spectra, Vol. 12, no. 4, pp. 845-862.

29. **SAP 2000** (2009). Integrated Software for Structural Analysis and Design, Version 14.0. Computers & Structures, Inc., Berkeley, California.

30. **Scrivener, J. C.** (1972), Reinforced masonry - seismic behaviour and design. Bulletin of the New Zealand National Society for Earthquake Engineering, vol. 5, no. 4, pp. 143-155

31. **SP 20 (S&T).** (1991). Code of Practice for Structural use of Un-reinforced Masonry, Bureau of Indian Standards, New Delhi.

32. **Tiany Yi**, **Franklin L Moon**, **Roberto T Leon** and **Lawrence F Kahn.** (2006). Analyses of a Two-Story Unreinforced Masonry Building. *Proceedings of ASCE (0733-9445)*, Paper 132:5(653).

33. **Tomazevic, M. (1999),** "*Earthquake Resistant Design of Masonry Buildings"*, Imperial college press, London.

LIST OF PAPERS SUBMITTED ON THE BASIS OF THIS THESIS

REFEREED JOURNALS

1. **Sar, D. R. and Sarkar, P. "**Pushover Analysis of Unreinforced Masonry Building", communicated to Structures, Elsevier Science.

PRESENTATION IN CONFERENCES

2. **Sar, D. R.** and **Sarkar, P.** (2012) "Seismic Evaluation of Un-Reinforced Masonry Building". *International Symposium on Engineering under Uncertainty: Safety Assessment and Management January 4 to 6 2012"*, January 4 to 6, 2012, Paper No. CNP 071, BESU, Shibpur, India.